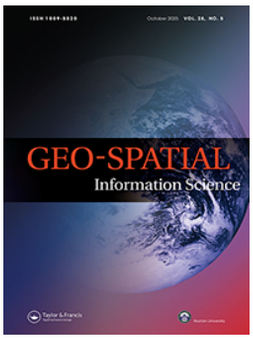

Geo-spatial Information Science

ISSN: 1009-5020 (Print) 1993-5153 (Online) Journal homepage: www.tandfonline.com/journals/tgsi20

How do humans navigate in the virtual lunar environment?

Bowen Shi, T. Qin, B. He, L. Mu & W. Dong

To cite this article: Bowen Shi, T. Qin, B. He, L. Mu & W. Dong (15 Sep 2025): How do humans navigate in the virtual lunar environment?, Geo-spatial Information Science, DOI: 10.1080/10095020.2025.2548954

To link to this article: https://doi.org/10.1080/10095020.2025.2548954

Published online: 15 Sep 2025.

GEO-SPATIAL INFORMATION SCIENCE
https://doi.org/10.1080/10095020.2025.2548954

Taylor & Francis
Taylor & Francis Group

How do humans navigate in the virtual lunar environment?

Bowen Shi [a,b], T. Qin [a,c], B. He [a], L. Mu [d] and W. Dong [a]

[a]Advanced Interdisciplinary Institute of Satellite Applications, State Key Laboratory of Earth Surface Processes and Hazards Risk Governance, Faculty of Geographical Science, Beijing Normal University, Beijing, China; [b]Department of Land Surveying and Geo-Informatics, The Hong Kong Polytechnic University, Hong Kong, China; [c]Research Group CartoGIS, Department of Geography, Ghent University, Ghent, Belgium; [d]Key Laboratory of Space Utilization, Technology and Engineering Center for Space Utilization, Chinese Academy of Sciences, Beijing, China

ABSTRACT

Exploring navigation strategies in lunar environment contributes to understanding the unique navigation mechanism of humans in extraterrestrial environments. However, it is unclear whether human navigation strategies in lunar environments are the same as those in common environments. In this study, a virtual lunar exploration navigation experiment was conducted. Participants were required to complete spatial learning, navigation, and destination-pointing tasks while their behavioral performance and scalp electroencephalogram (EEG) data were recorded. The navigation trials (88 trials from 62 participants) were divided into two groups – path retracing strategy ($N = 60$, navigating along the known routes) and path integration strategy ($N = 28$, inferring potential shortcuts) groups – and differences in navigation performance and brain workload between them were measured. Results indicated that trials using the path integration strategy were more efficient in terms of time cost and pointing error. Particularly, navigators using the path integration strategy were adaptive in their brain workload. Their EEG theta power spectral density (PSD) metrics differed for routes with different difficulties; this difference was not found in the path retracing group. This study offers insights into human navigation strategies and cognitive processes in virtual lunar scenes and contributes to future human adaptation to the lunar surface environment when conducting space missions.

ARTICLE HISTORY
Received 28 October 2024
Accepted 12 August 2025

KEYWORDS
Lunar environment; navigation strategy; theta power; EEG

1. Introduction

During goal-directed activities, such as hunting, exploration, and commuting, humans have evolved various navigation strategies to reach specific destinations (Goodroe and Spiers 2022). These strategies have been effectively utilized across diverse terrestrial environments, from structured spaces such as urban and rural road networks to unstructured terrains like forests, mountains, and deserts. As manned space technology advances, understanding how humans navigate in extraterrestrial settings – particularly the lunar environment – is therefore crucial for planning future space exploration and habitation missions. Individuals employing different strategies acquire and utilize spatial knowledge in distinct ways. Previous studies have categorized navigation strategies according to the type of spatial knowledge employed (Maier et al. 2024; Marchette, Bakker, and Shelton 2011; Wiener et al. 2013). These strategies have been investigated and validated in virtual environments through assessments of navigators' behavioral performance and cognitive processes (Gramann et al. 2010). In the first strategy, navigators typically retrace their paths via stimulus-response actions, relying on learned landmark and route knowledge. Conversely, those employing the alternative strategy construct allocentric cognitive maps to plan novel routes and continuously update their position and orientation via path integration (Hegarty et al. 2022). We herein designate these strategies as the "path retracing strategy" and the "path integration strategy" for clarity and specificity. Unlike common navigation scenarios, lunar settings lack tools such as satellites and compasses, with limited landmark cues. Thus, whether humans can adapt similar navigation skills and strategies as those of Earth – particularly in virtual simulations – remains an open question and requires further investigation.

Previous studies have investigated behavioral and cognitive metrics, including time cost (Santos-Pata and Verschure 2018), pointing error (Barhorst-Cates, Rand, and Creem-Regehr 2016), and EEG-based theta band power (Plank et al. 2015), in spatial learning and navigation tasks involving path retracing and path integration strategies. Regarding behavioral performance, participants employing the path integration

CONTACT W. Dong dongweihua@bnu.edu.cn

strategy exhibited shorter time costs and lower pointing errors in virtual mazes (He, Boone, and Hegarty 2023). Accordingly, we hypothesized that participants using the path integration strategy would demonstrate superior performance in navigation and destination-pointing tasks within virtual lunar scenes (Hypothesis 1a). However, given the increased difficulty in identifying shortcuts amid sparse lunar landmarks, we anticipated that this strategy might not be the predominant choice for navigators (Hypothesis 1b). Furthermore, previous research has revealed greater theta band activation in large-scale virtual environments during the retrieval of allocentric cognitive maps (Teixeira De Almeida et al. 2023). Given the associations between path integration and cognitive map formation, we thus hypothesized that participants employing the path integration strategy would exhibit greater theta band activation in virtual lunar scenes (Hypothesis 2).

To test these hypotheses, we conducted an experiment in a virtual lunar exploration environment, comparing the impacts of navigation strategies on behavioral performance and brain workload. Participants wore a mobile EEG system during spatial learning, navigation, and destination-pointing tasks. For a comprehensive analysis of navigation strategies, we extracted behavioral performance and brain workload metrics, augmented by self-reported scale scores. This study aimed to summarize the behavioral performance and cognitive processes underlying distinct navigation strategies in virtual lunar settings, thereby furnishing foundational insights for extraterrestrial human exploration missions.

2. Related work

2.1. Navigation strategies for various scenes

The path retracing and path integration strategies differ with respect to navigators' inclinations toward shortcut-seeking and their utilization of spatial knowledge, including landmark, route, and survey knowledge (Siegel and White 1975). The path retracing strategy, which is dominated by habit-driven processes, relies on landmark and route knowledge. It emphasizes stimulus-response action sequence along the navigation route but does not consider the spatial relationships between landmarks and routes (Gardner et al. 2016). In contrast, the path integration strategy integrates landmark and path knowledge into cognitive maps to establish survey knowledge (Tolman 1948). Navigators with this strategy use a cognitive map to determine the optimal route by inferring the relative spatial relationships between themselves and their destinations. Behaviorally, the path retracing strategy tends to involve familiar landmarks and routes, whereas the path integration strategy may involve identifying novel shortcuts. Previous studies on the neural basis of navigation tasks illustrated the specific activation of the two navigation strategies in different brain regions. Pioneering animal studies have revealed that place cells (O'Keefe and Dostrovsky 1971), head direction cells (Taube, Muller, and Ranck 1990), and grid cells (Hafting et al. 2005) in the hippocampus and entorhinal cortex encode Euclidean space, forming the neural basis of the cognitive map and path integration strategy. The path retracing strategy is driven by the caudate-putamen in the striatum (Packard and McGaugh 1996). The outputs of these brain regions are modulated by the prefrontal cortex and together influence the navigation strategies of animals (Chersi and Burgess 2015).

Navigation processes are influenced by interactions among navigators' spatial knowledge, navigation strategies, and environmental characteristics (Brunyé et al. 2017). In small-scale experimental scenes, such as virtual mazes within limited boundaries, studies have revealed differences in the use of shortcuts between the two strategies, and the navigation strategies correspond to activation in different brain regions (Anggraini, Glasauer, and Wunderlich 2018; Bohbot et al. 2012). In large-scale experimental scenes, such as virtual towns, forests, and deserts, humans usually use landmark information for navigation (Yesiltepe, Conroy Dalton, and Ozbil Torun 2021). Landmark saliency (Steck and Mallot 2000) and reliability (Foo et al. 2005; Zhao and Warren 2015) affect individuals' dependence on different types of spatial knowledge and thus affect navigation strategies. In addition, navigators' preferences for relying on egocentric and allocentric spatial references during navigation tasks influence navigation strategies. Specifically, those who use a path retracing strategy tend to use egocentric reference frames, whereas those who use a path integration strategy are more likely to plan navigation routes based on allocentric reference frames (Hegarty et al. 2022). Note that different spatial references may exist simultaneously in the large-scale navigation process through integration and conversion (Ekstrom, Arnold, and Iaria 2014; Wiener, Kmecova, and Condappa 2012). We thus differentiate navigation strategies instead of spatial reference frames based on behavioral performance in experimental scenes with high ecological validity.

Unlike the Earth environment, the lunar surface presents unique landscapes, such as impact craters and expansive plains, with landmark cues that are simpler than those of the Earth. Investigating human navigational behaviors and cognitive processes in the virtual lunar environments can offer valuable insights for future long-term extraterrestrial exploration and

habitation. Therefore, this study introduced a large-scale, high ecological validity lunar surface simulation to explore human navigation strategies.

2.2. Behavioral performance, cognitive load, and brain workload measurement method

Measuring navigators' behavioral performance is crucial for understanding the differences in behavior among users of different navigation strategies. In small-scale maze environments, the proportion of trials involving shortcut usage has been evaluated to quantify the preferences between the two navigation strategies (Marchette, Bakker, and Shelton 2011). The time cost and trajectory length are commonly used to assess the efficiency of navigation (Santos-Pata and Verschure 2018). The path integration strategy is frequently linked to shorter time and distance costs, owing to effective shortcut employment. To evaluate mastery of survey knowledge, researchers have used pointing tasks and analyzed pointing errors between the pointing direction and the destination direction (Barhorst-Cates, Rand, and Creem-Regehr 2016; He, Boone, and Hegarty 2023). Beyond behavior metrics, certain studies have quantitatively analyzed trajectories using morphological metrics, such as heading direction errors (Smith, McKeith, and Howard 2013) and trajectory circuity Ballou, Rahardja, and Sakai (2002). These metrics can be used to measure the degree to which a route detours to destination and thus to infer navigation performance. Spatial ability, which has been proven to influence navigation strategy and performance (Riecke, Veen, and Bülthoff 2002; Schug 2016), has been quantified by a series of self-reported scales, such as the Santa Barbara Sense of Direction scale (SBSOD) (Hegarty et al. 2002) and the spatial anxiety scale (Lawton 1994).

The cognitive load is linked to the workload in navigation tasks. Previous studies have measured cognitive load via scales, physiological and brain metrics. The cognitive load scales focus on participants' self-reports of task performance, effort, time pressure, mental pressure, physical workload, negative emotions, and other factors (Paas and Van Merrienboer 1993; Reid et al. 1988), represented by the NASA Task Load Index (NASA-TLX) scale (Hart and Staveland 1988). Physiological metrics, including heart rate variability (Christensen and Wright 2014), the galvanic skin response (Yang et al. 2021), eye blinks (Kosch et al. 2018; Nourbakhsh, Wang, and Chen 2013; Zheng et al. 2012), and pupil dilation (Condappa and Wiener 2014; Yang and Kim 2019), are commonly used to assess the level of effort and stress levels in tasks. EEG-derived brain signals provide a more interpretable representation of cognitive processes compared to physiological data by combining the cognitive function across various cerebral cortical regions, which can explain the variation in brain workload, including cognitive load, learning process, attention allocation, and working memory (Miyakoshi et al. 2021; Paas et al. 2003; Saitis and Kalimeri 2016). Specifically, frontal theta band waves are associated with human cognitive control processing (Cavanagh and Frank 2014) and working memory (Gevins and Smith 2000; Kahana, Seelig, and Madsen 2001). Chrastil et al. (2022) reported that participants undertaking complex tasks in virtual environments presented greater frontal theta power. In addition, the increasing task load leads to theta and alpha oscillations in the occipital region (Cheng et al. 2022).

In the large-scale lunar environment, characterized by sparse landmarks and absent satellite-based navigation, navigators must undertake complex spatial learning and navigation decisions. Accordingly, we extracted behavioral performance and brain workload metrics to comprehensively understand the differences in navigation strategies in the virtual lunar environment. In addition, time series analysis of behavioral and EEG data was applied to explore the navigators' behavioral and cognitive processes during the tasks.

3. Methodology

3.1. Experiments and data collection

To explore behavioral and cognitive processes during spatial navigation tasks, previous research has commonly conducted experiments in virtual scenes (Cornwell et al. 2008; Weidemann, Mollison, and Kahana 2009). Hence, a scenario was established for future manned lunar exploration missions, with the assumption that a lunar rover departs from a lunar exploration base and autonomously explores the lunar surface (Figure 1(a)). In the case of a loss of satellite signals, manual control is required for the rover to return to the lunar base and deliver soil samples. The participants completed three experimental tasks: spatial learning, navigation, and destination-pointing. During these complex tasks, the behavioral and cognitive data of the participants were recorded. Unlike functional MRI (fMRI), which presents stimuli only in the form of static images or videos, EEGs have been used to measure participants' cerebral cortex signals in many existing studies of large-scale high ecological validity scenes (Caplan et al. 2003; Liu, Singh, and Lin 2022). Hence, the EEG tool was applied to record and measure the brain workload metrics.

3.1.1. Experimental setups

First, a virtual lunar terrain model was built based on lunar observation data. The selected experimental area on the lunar surface is located between 44.1°N – 44.2°N and 64.5°E – 64.6°E, forming a rectangular region approximately 5.8 km long and 4.5 km wide

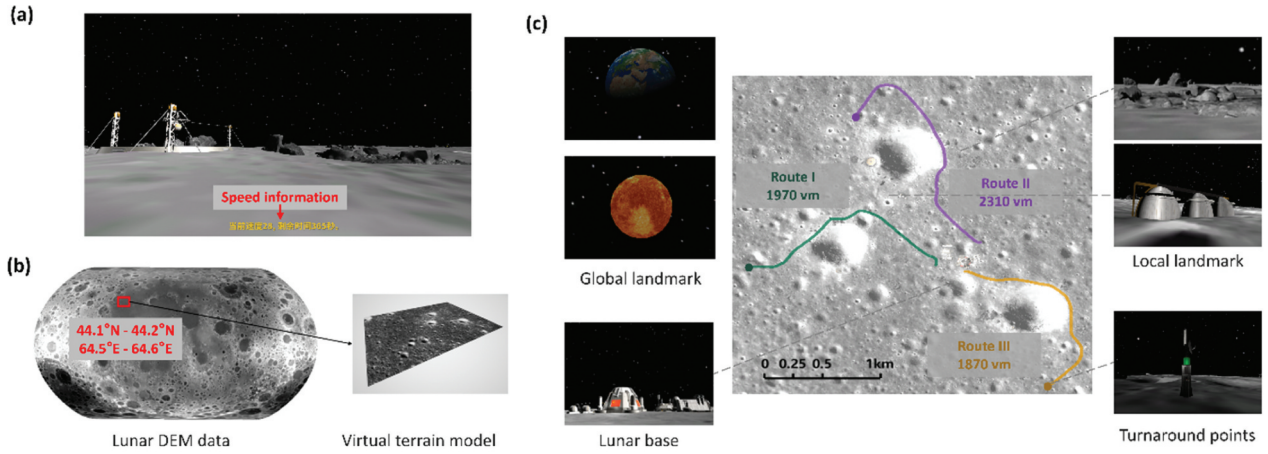

Figure 1. Experimental scene setups. (a) Virtual lunar exploration interface. (b) Illustration of the experimental area. The DEM data of the experimental area were transformed into a virtual terrain model. (c) Illustration of the three experimental routes, which ranged in length from approximately 1900 to 2300 virtual meters (vm). In the virtual lunar scene, global landmarks, local landmarks, the lunar base, and turnaround points were placed to provide spatial cues for the participants.

(Figure 1(b)). The terrain is predominantly flat, but several large ringed mountains and small impact craters are interspersed in this lunar region. Local visibility conditions are suboptimal; thus, the difficulty level for spatial cognition tasks is moderate. Based on the lunar digital elevation model (DEM) data, we developed a virtual simulation experiment system within the Unity 3D 5.0 engine to support spatial cognition tasks.

In this experimental system, participants can navigate the lunar virtual environment by performing forward and backward movements, making turns and climbing slopes, exploring the terrain, and performing navigation tasks. To simulate the turning and climbing performance of a lunar rover in a natural lunar exploration environment, we configured the mobility settings of the virtual lunar rover within the virtual system and imposed specific limitations on its turning angular velocity and climbing capabilities. During the experiment, the participants could monitor the rover's speed in real-time.

As shown in Figure 1(c), we designed three navigation routes with an average length of 2050 virtual meters. These routes started from the lunar base located at the center of the experimental area and extended toward three different lunar craters in the west, north, and southeast directions, respectively, followed by a detour before they reached the turnaround points. To enrich the spatial cues of the scene, a series of landmarks were integrated into the virtual scene. According to Steck and Mallot (2000), these landmarks included navigation start and end points (depicting the location of the lunar base and the route turnaround point), global landmarks (visible within the whole area and providing stable directional cues for navigators), and local landmarks (visible within a limited area, located on either side of the navigation route, and offering participants small-scale spatial cues).

3.1.2. Participants

62 participants—42 females and 20 males – aged 18–30 years ($M = 22.53$, $SD = 2.67$) were recruited from the college for the virtual simulation experiment. These participants were selected from a total of 165 applicants based on their answers to a questionnaire that investigated their thorough understanding of the experimental tasks and spatial navigation abilities that were necessary for the experiment. All participants had normal or corrected-to-normal vision and no astigmatism.

3.1.3. Experimental procedure

As shown in Figure 2(a), after arriving at the laboratory, each participant confidentially provided demographic information, including gender and age, via an online questionnaire. The participants were then granted access to the virtual simulation experiment system and familiarized themselves with basic operations, such as forward and backward movements and turning left and right. Additionally, the experimenter provided a detailed overview of the experimental procedure to ensure that the participants thoroughly understood the experiment. To minimize the impact of learning effects, the practice virtual environment closely mirrored the formal experimental setting in terms of terrain and environmental features but had distinct landmark cues. After the resting-state EEG data were collected, the participants were randomly allocated to undertake two individual trials among three routes, with approximately 3 min of rest between the two trials. Within each trial, the participants were required to perform three tasks:

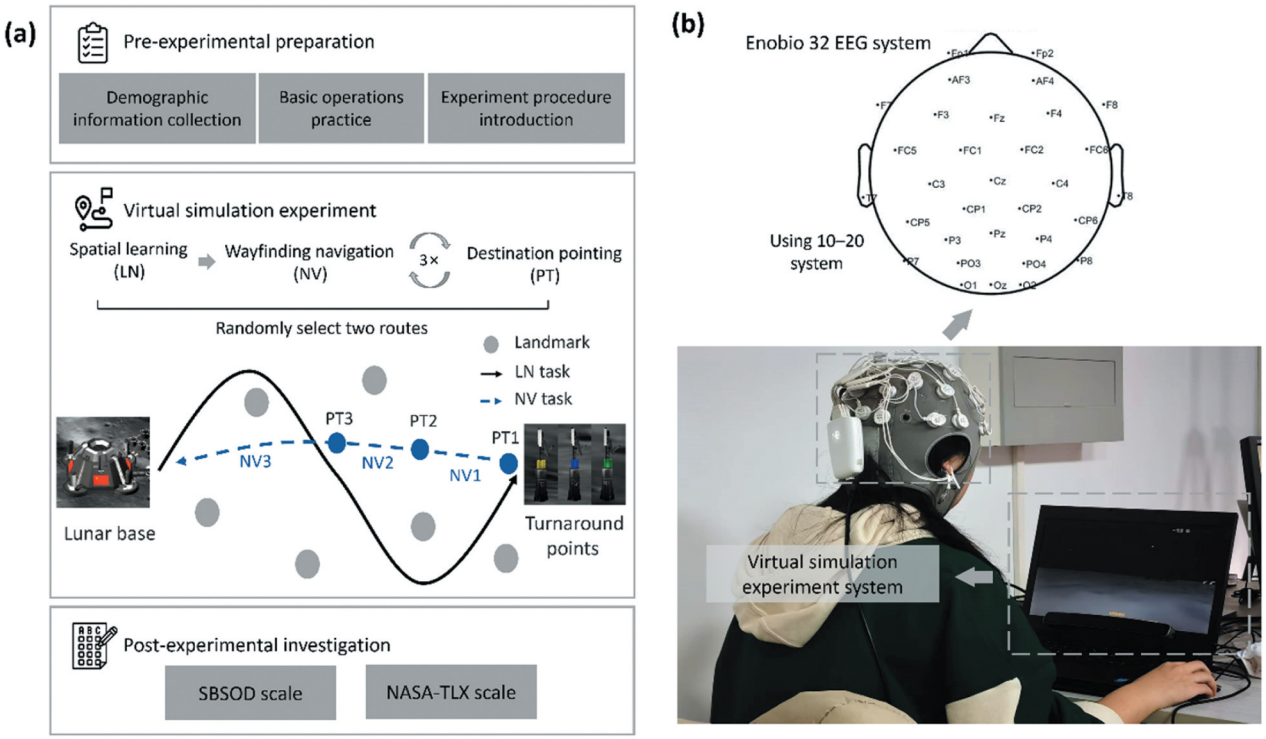

Figure 2. Experimental procedure and experimental scene. (a) Experimental procedure. The participants were required to complete three tasks in each virtual simulation experiment trial, as illustrated below (LN: spatial learning, NV: navigation, PT: destination-pointing). (b) Experimental scene in the laboratory and EEG electrode distribution (32 electrodes according to the 10–20 system).

3.1.3.1. Spatial learning (LN) task. Participants passively traversed predefined exploration routes on the lunar surface toward the turnaround points. The participants could not move forward or backward throughout the route, but could rotate their viewpoint to observe the landmarks along the route and were instructed to memorize the route and direction. The participants could replay the completed routes until they felt that they had fully learned spatial knowledge.

3.1.3.2. Navigation (NV) task. After completing the LN task and reaching the turnaround points, the participants were instructed to utilize their acquired spatial knowledge to plan the shortest homing route to the lunar base without maps or satellite navigation. Note that the routes in the LN task were not the shortest ones. Instead, the NV task encouraged participants to explore homing shortcuts on the other side of the crater to examine the participants' preferences between the path retracing and path integration strategies. Throughout the task, the lunar base was mostly hidden from view until the participants reached the final stage, when the lunar base's structures were displayed. The task was deemed unsuccessful if a participant failed to navigate back to the base within 400 s.

3.1.3.3. Destination-pointing (PT) task. Participants performed three PT tasks during the NV task. In each task, the participants were required to rotate the rover in the direction of the lunar base while it remained invisible. The system automatically recorded the time cost and pointing error. Based on the distance between the real-time individual position of the participant and the location of the lunar base, the participants completed three pointing tasks at positions 100%, 75%, and 50% of the total distance. These task phases are referred to as PT1, PT2, and PT3, respectively. Additionally, each navigation task phase was separated into three PT tasks, which were named NV1, NV2, and NV3.

After completing two trials, the participants completed the online scales, including the Santa Barbara Sense of Direction scale (SBSOD) (Hegarty et al. 2002) and the NASA-TLX (Hart and Staveland 1988). These two representative scales were widely applied to collect feedback on participants' spatial ability and cognitive load (Fabroyir and Teng 2018; Taillade, N'Kaoua, and Sauzéon 2016). In the SBSOD scale, participants self-evaluate their spatial abilities across 15 dimensions. The NASA-TLX scale prompted participants to self-evaluate the cognitive load across six dimensions (including mental demand, physical demand, temporal demand, performance, effort, and frustration level) for the two completed routes and assign weights to six dimensions relative to their importance.

The experiment was conducted in an indoor laboratory. The experimental scene is shown in Figure 2(b). The virtual simulation experiment system was run on

a laptop computer (Intel Core i7 4900MQ CPU 2.80 GHz, with a screen size of 34.6 × 1080 and a screen resolution of 1920 × 1080). EEG data from the participants were collected by the Enobio 32 EEG system at a sampling rate of 500 Hz. The cortical electrical signals were acquired from 32 evenly distributed electrodes across the scalp. The EEG signals had a sampling bandwidth of 0–125 Hz, covering the brain signal bandwidth, with a reference electrode placed at the participant's right mastoid. Before the EEG data were recorded, the impedance of the electrodes was checked. For most electrodes, the impedances were kept below 10 kΩ, whereas a few were between 10 and 15 kΩ. The EEG data acquisition process was controlled by the NE NIC2 2.0.11 software. All the data acquisition devices were connected to a laptop. The event markers were manually annotated at the beginning and end stages of the experiment to facilitate subsequent data processing and ensure the synchronization of multiple data streams. The alignment was based on the markers recorded during the experimental process. The time discrepancy between all the data points was confirmed to be less than 100 ms.

Ethical approval for this study was obtained from the Ethics Committee of Beijing Normal University before the experiment (approval document number: 202304070068). Before the formal experiment commenced, all the participants signed informed consent forms and were informed that they could terminate the experiment at any time if they felt uncomfortable. The entire experimental procedure lasted approximately 45–50 min for each participant. After finishing the experiment, each participant received a payment of 150–180 CNY (approximately 21–25 USD), which was correlated with their experimental performance.

3.2. Data processing and analysis

3.2.1. Behavioral performance and trajectory morphology metrics

A total of 124 trials were conducted by 62 participants (with two trials for each participant). However, since the participants in some trials failed to reach the destination within the time limit (Figure A1), only 88 trials were considered for further analysis. These 88 trials were divided into two strategy group:

- Path retracing group (PR): Participants selected the original route (i.e. the longer, superior arc along the crater rim) to return to the lunar base during the navigation (NV) task.
- Path integration group (PI): Participants chose a shortcut (i.e. the shorter, minor arc across the crater) to return to the lunar base during the NV task.

The distribution of trials in each route and strategy group is presented in Figure 3(a). Overall, the number

(a)

Route I		Route II		Route III		Total	
Group	N	Group	N	Group	N	Group	N
PR	18	PR	22	PR	20	PR	60
PI	11	PI	7	PI	10	PI	28
Total	29	Total	29	Total	30	Total	88

(b)

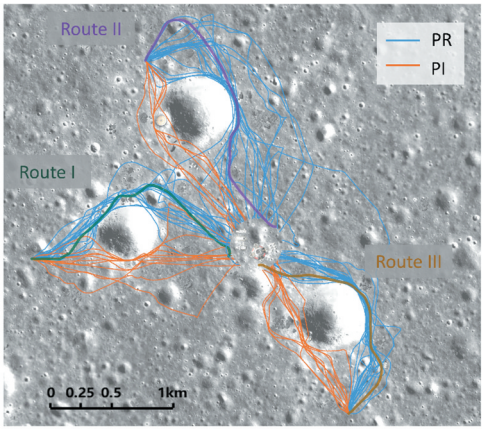

Figure 3. Participants were divided into "path retracing strategy (PR)" and "path integration strategy (PI)" groups. (a) Number of trials in each route and each group. (b) Navigation trajectories in the NV task.

of trials for the three routes was consistent, with approximately two-thirds of the trials involving the path retracing strategy. In these cases, the participants tended to navigate to the lunar base following the route learned in the LN task. The navigation trajectories are shown in Figure 3(b). Owing to the deliberately designed detour in the passive navigation route learned by participants in the LN task, there was a divergence in their decision-making during the return trip. Furthermore, since the participants were informed during the practice phase that the lunar rover had limited climbing capabilities, all participants opted to circumvent the circular mountains to avoid traversing areas with steep slopes.

In addition, we examined the demographic properties and found no statistically significant differences in the participants' age ($t(86) = -0.314$, $p = 0.754$) or gender ($t(86) = -0.064$, $p = 0.949$) between the two groups. Therefore, the distributions of both age and sex between the two groups were deemed statistically consistent. As a result, in subsequent analyses, it was unnecessary to consider demographic attributes as covariates.

To evaluate the participants' performance in the virtual simulation experiments, we computed five unique behavioral metrics, including three performance metrics and two trajectory morphological metrics (Table 1). For the time cost (TC) and trajectory length (TL) metrics, we conducted a two-way ANOVA using a factorial design of 2 (strategy group: PR vs. PI) × 3 (route: route I vs. II vs. III). For the pointing error (PE) metric, we conducted a three-way ANOVA via a factorial design of 2 (strategy group: PR vs. PI) × 3 (route: route I vs. II

Table 1. Behavioral metric definitions.

Indicator		Definition
Performance indicators	Time cost (TC)	The reaction time used for finishing LN, NV, and PT tasks.
	Trajectory length (TL)	The length of the return trajectory in the NV task.
	Pointing error (PE) (Barhorst-Cates, Rand, and Creem-Regehr 2016)	The angle between the participants' pointing direction and the actual destination direction for the PT1, PT2, and PT3 tasks.
Trajectory morphology indicators	Heading error (HE) (Smith, McKeith, and Howard 2013)	The angle between the return trajectory heading and the participants' pointing direction towards the destination for NV1/PT1, NV2/PT2, and NV3/PT3 tasks.
	Circuity (CR) (Ballou, Rahardja, and Sakai 2002)	Trajectory length divided by the Euclidean distance.

vs. III) × 3 (task phase: PT1 vs. PT2 vs. PT3). For the heading error (HE) and circuity (CR) metrics, we conducted a three-way ANOVA via a factorial design of 2 (strategy group: PR vs. PI) × 3 (route: route I vs. II vs. III) × 3 (task phase: NV1 vs. NV2 vs. NV3). All the main effects and interaction effects of the independent variables were examined. For the significant effects, we further performed a post-hoc T-test.

3.2.2. Scale scores

The reliability of the scale score data was assessed via Cronbach's α coefficient. The results indicated high reliability for the SBSOD and NASA-TLX scales, with Cronbach's α values of 0.922 and 0.737, respectively. Subsequently, Pearson's correlation coefficient was employed to examine the correlation between the scale scores and TC metrics in the NV/PT tasks. We also explored the correlation between TC and the scores for individual questions at both scales. The SBSOD score was analyzed at the participant level ($N = 62$), whereas the NASA-TLX score was analyzed at the trial level ($N = 88$).

3.2.3. EEG-based brain workload metric

For the preprocessing of EEG signals, we initially imported the raw EEG data and determined the positions of 32 electrodes according to the 10–20 system. We subsequently employed the average potential of all 32 electrodes as the reference electrode and re-referenced the raw data. A bandpass filter ranging from 0.1 Hz to 80 Hz was applied to eliminate noise signals outside the brain signal frequency domain. Additionally, a notch filter from 47 Hz to 53 Hz was used to effectively attenuate power line signals centered at approximately 50 Hz. Noise artifacts associated with eye blinks, head movements and muscle activity were manually identified and removed via independent component analysis (ICA) (Vigário 1997).

We performed a time-frequency analysis for each EEG event via the Morlet wavelet transform by mapping the EEG waveforms in the 1–27 Hz frequency range from the time domain to the frequency domain. Following previous literature, the number of cycles for the Morlet wavelet was set to 3. Relative theta power is a commonly used EEG metric (Bian et al. 2014; Cheng et al. 2022). Referring to previous studies, we subsequently extracted the relative theta power for each event based on the power spectral density (PSD) via the following equation:

$$P = \frac{P_{\text{theta}}}{P_{\text{delta}} + P_{\text{theta}} + P_{\text{alpha}} + P_{\text{beta}}} \quad (1)$$

where P represents the relative theta power, and P_{delta}, P_{theta}, P_{alpha}, and P_{beta} denote the power values corresponding to the delta (1–3 Hz), theta (4–8 Hz), alpha (9–13 Hz), and beta wavebands (14–27 Hz), respectively.

Statistical analysis was performed using the relative theta PSD of 32 electrodes across the whole brain. We first conducted a three-way ANOVA using a factorial design of 2 (strategy group: PR vs. PI) × 3 (route: route I vs. II vs. III) × 3 (task phase: LN vs. NV vs. PT) to detect main effects and interaction effects. Considering the intersubject variability and nonnormal distribution of the data, before the ANOVA test, we applied a square root transformation to mitigate the skewness of the data. Furthermore, we employed a threshold of three times the median absolute deviation (MAD) to remove outliers. We subsequently created a temporal sequence by partitioning the LN and NV tasks into 40 time bins consisting of 20 bins for LN, 5 for NV1, 5 for NV2, and 10 for NV3. At each time bin, we conducted T-tests to explore the differences in the relative theta PSD among participants and qualitatively examined the temporal dynamics of the relative theta PSD. Finally, Spearman correlation analyses were conducted to assess the relationships between the relative theta PSD and the morphological metrics of the two trajectories.

The data analysis process reported in this section was conducted with the EEGLAB 14.1.1 toolbox (Delorme and Makeig 2004), MNE-Python 1.3.0 (Gramfort et al. 2013), FieldTrip toolbox (Oostenveld et al. 2011), SPSS 26 (IBM 2019), and Psychometrica (Lenhard and Lenhard 2022).

4. Results

4.1. Behavioral performance and trajectory morphological results

We observed a significant main effect of strategy on time cost (TC) in the NV task ($F(1,86) = 28.681$, $p <$

0.001; effect size $f = 1.201$, Figure 4(a)). Additionally, the post-hoc T-test revealed significant differences between the two strategies ($p < 0.001$), indicating that the path integration group required less time to finish the NV task than the path retracing group did. The TC differences were significant for route II ($p < 0.001$) and route III ($p < 0.01$), and there was a similar pattern in route *I*, but not statistically significant (Figure 4(b)). However, no significant main or interaction effects were found on the TC metric of the LN and PT tasks.

Figure 4(c) displays the ANOVA results for the trajectory length (TL) metric and shows significant main effects of strategy ($F(1,86) = 64.063$, $p < 0.001$; $f = 0.836$) and route ($F(2,85) = 7.615$, $p < 0.001$; $f = 0.429$)

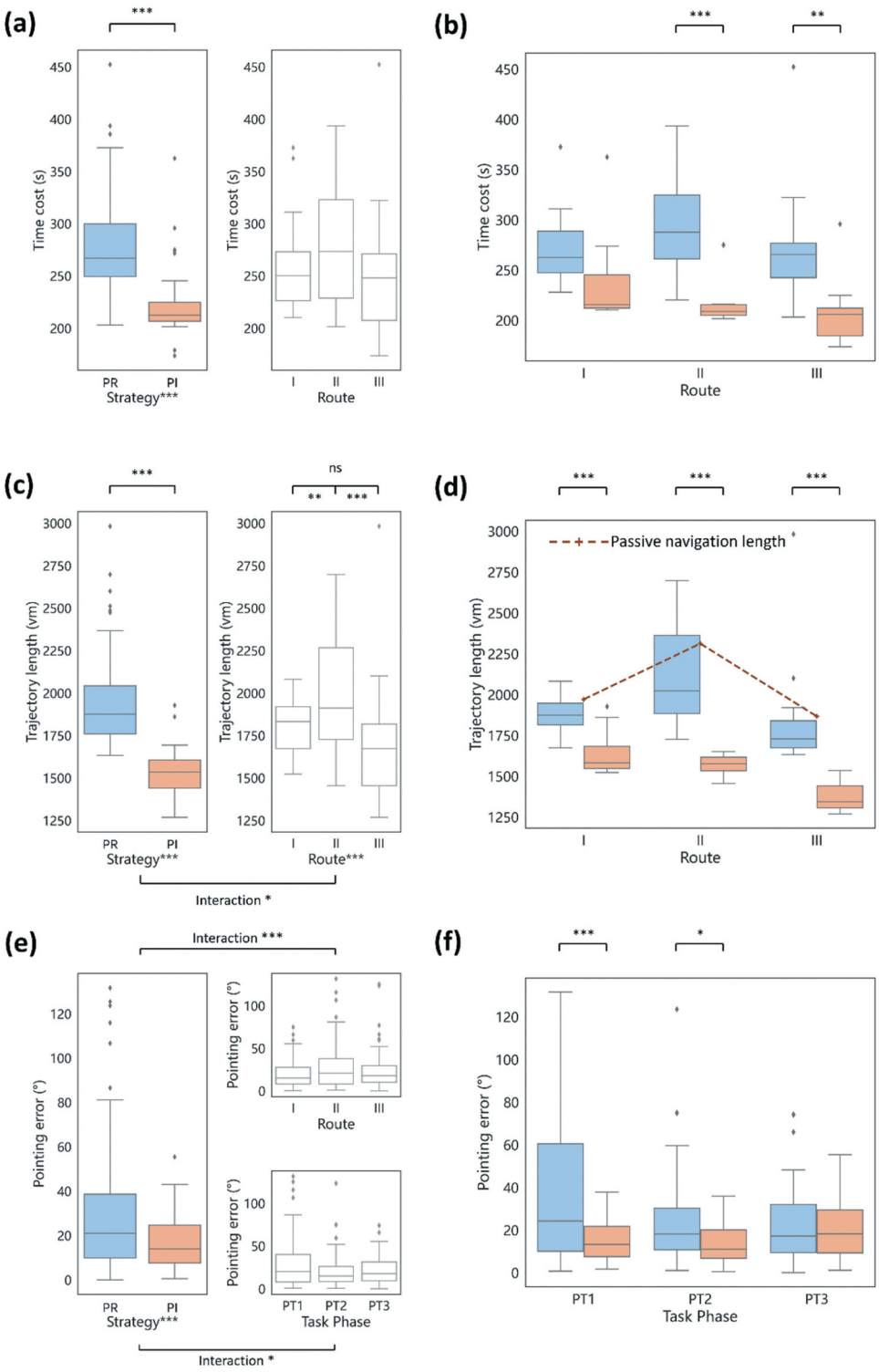

Figure 4. ANOVA results of the performance metrics. (a) The main effects of the time cost metric in the NV task. (b) The strategy×route interaction effect of the time cost metric in the NV task. (c) The main effects of the trajectory length metric. (d) Stratexgy×route×route interaction effect of the trajectory length metric. (e) The main effects of the pointing error metric. (f) The strategy×task phase interaction effect of the pointing error metric. (The blue boxes represent the path retracing (PR) group, and the orange boxes represent the path integration (PI) group. * $p < 0.05$, ** $p < 0.01$, *** $p < 0.001$).

along with asignificant interaction effect between the two factors ($F(5,82) = 3.205$, $p < 0.05$; $f = 0.968$). We explored the interaction effect between strategy and route (Figure 4(d)). The TL metric of the path integration group is significantly shorter for all three routes ($p < 0.001$). Qualitatively, the TL of the path retracing group was closer to the passive navigation route in the LN task, whereas the TL of the path integration group exhibited significant differences due to shortcuts.

Figure 4(e) displays the ANOVA results for the pointing error (PE) metric. We observed asignificant main effect of strategy ($F(1,260) = 17.772$, $p < 0.01$; $f = 0.256$), and the post-hoc T-test revealed significant differences between the two strategies ($p < 0.001$), indicating that the path integration group performed significantly better than the path retracing group did in the PT task. Additionally, we observed asignificant interaction effect between strategy and task phase ($F(5,256) = 3.529$, $p < 0.05$; $f = 0.313$). We found that the PE of the path retracing group was significantly greater than that of the path integration group in the PT1 ($p < 0.001$) and PT2 ($p < 0.05$) phases, but the difference was not significant in the PT3 phase (Figure 4(f)).

Figure 5(a) displays the ANOVA results for the heading error (HE) metric. We observed asignificant main effect of strategy ($F(1,260) = 7.341$, $p < 0.01$; $f = 0.179$), and the post-hoc T-test revealed significant differences between the two strategies ($p < 0.01$), indicating that the path integration group was more inclined to navigate in the pointing direction. In contrast, the path retracing group tended to travel with greater angular offsets. We explored the interaction effect between the strategy and task phases (Figure 5(b)). The HE of the path retracing group was significantly greater than that of the path integration group in the NV2 phase ($p < 0.05$).

Figure 5(c) displays the ANOVA results for the circuity (CR) metric. We observed asignificant main effect of the strategy ($F(1,255) = 15.316$, $p < 0.001$; $f = 0.228$). Post-hoc T-tests revealed asignificant difference between the CRs of the two strategy groups ($p < 0.001$). In particular, we focused on the interaction effect between the strategy and task phases ($F(5,251) = 3.778$, $p < 0.05$; $f = 0.262$, Figure 5(d)). The CR of the path retracing group was significantly greater than that of the path integration group in the NV1 phase ($p < 0.001$) and the NV2 phase

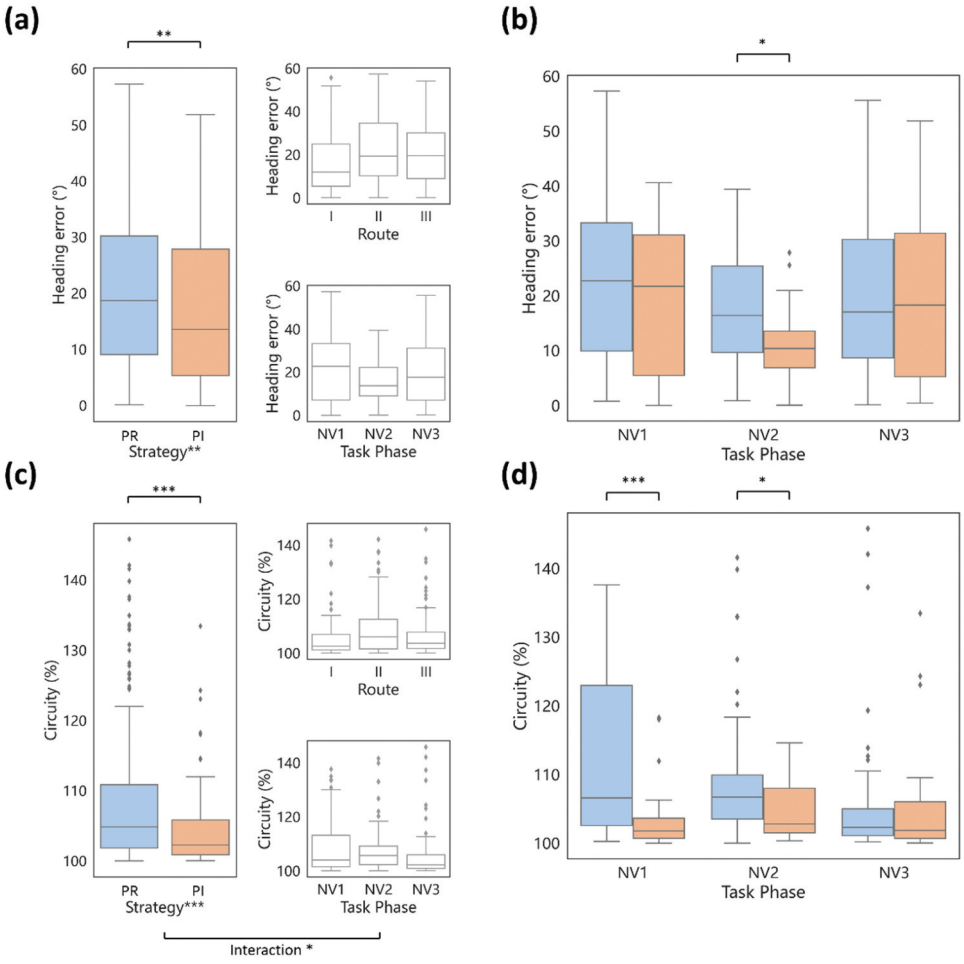

Figure 5. ANOVA results of trajectory morphological metrics. (a) ANOVA results of the heading error metric. (b) Strategy×task×task phase interaction effect of the heading error metric. (c) ANOVA results for the circuity metric. (d) Strategy×task×task phase interaction effect of the circuity metric. (the blue boxes represent the path retracing (PR) group, and the orange boxes represent the path integration (PI) group. *$p < 0.05$, **$p < 0.01$, ***$p < 0.001$).

($p < 0.05$). However, in the NV3 phase, there was no significant difference between the two groups, indicating that the morphological differences mainly appeared in the first half of the NV task.

The detailed data that supported the T-test results in this section can be found in Table A1.

4.2. Scale score results

The correlation analysis revealed asignificant negative correlation between the SBSOD score and the total time cost of NV and PT ($r = -0.282$, $p < 0.05$) (Figure 6 (a)). Additionally, the exploratory analysis indicated that the TC correlated with the participants' feedback for Q8 ("I have no difficulty understanding directions") ($r = -0.252$, $p < 0.05$), Q9 ("I am good at reading maps") ($r = -0.336$, $p < 0.01$), Q14 ("I usually remember anew route after walking it once") ($r = -0.336$, $p < 0.01$), and Q15 ("I have agood mental map of my environment") ($r = -0.318$, $p < 0.05$). However, the significance of the individual question correlations could not be corrected by the FDR (Table A2) . Similarly, the NASA-TLX score was significantly correlated with the total TC of the NV and PT tasks ($r = 0.358$, $p < 0.001$) (Figure 6(b)). Further exploration revealed asignificant correlation between the "performance" score and TC ($r = 0.287$, $p < 0.05$, FDR-corrected, Table A2).

4.3. EEG-based brain workload results

We first tested the correlation between NASA-TLX scores (covering six dimensions: mental demand, physical demand, temporal demand, performance, effort, and frustration level) and the relative theta power during the tasks. We found 26 of 32 electrodes correlated with the "physical demand" component of the NASA-TLX score ($p < 0.05$, FDR-corrected, Table A3). In addition, we observed a significant interaction effect between strategy and route for 16 out of 32 electrodes (Figure 7(a,b)) and

Table A4 , $p < 0.05$ FDR-corrected). The electrodes with significant interaction effects were clustered into regions of interest (ROIs) based on the f values. Considering the spatial adjacency of the electrodes, these electrodes were divided into three ROIs, including the frontal region (F4, AF4, F8, and FC6), temporal region (T7, CP1, and CP5), and parietal region (Pz, PO3, and PO4). The interaction effects were further analyzed in these three regions, as shown in Table 2 and Figure 7(c)–(e). The relative theta PSD on three ROIs between the two strategies exhibited significant differences on route I (PR > PI). However, the relative theta PSD associated with the frontal region for individuals in the path integration group on route II was significantly greater than that for individuals in the path retracing group. Finally, the ROI did not significantly differ between the two groups on route III. We also performed the electrode-by-electrode t-tests on these ROIs, and the results were presented in Figure A3-A5. We observed some significant differences at individual electrodes that were not evident at the ROI level, such as the CP5 electrode in route III (theta PSD: PR > PI, Figure A4, left plot) and the T7 and CP1 electrodes in route II (theta PSD: PR < PI, Figure A4, middle and right plot).

We conducted a time series analysis on the whole-brain average relative theta PSD, focusing on route I as a case study (Figure 7(f)). Overall, we observed that the path retracing group resulted in a greater theta power, with significant differences primarily concentrated in the middle phases of the LN task and the NV task (NV2), whereas no significant differences were found in other task phases. Through temporal analysis, we found an upward trend in the brain workload for the path retracing group during the NV2 phase.

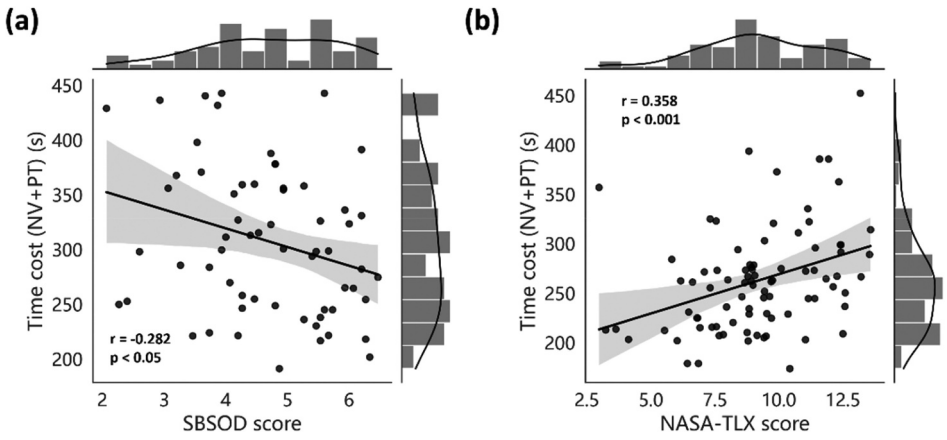

Figure 6. Correlation analysis results between the total time cost of the NV & PT tasks and (a) SBSOD score and (b) NASA-TLX score.

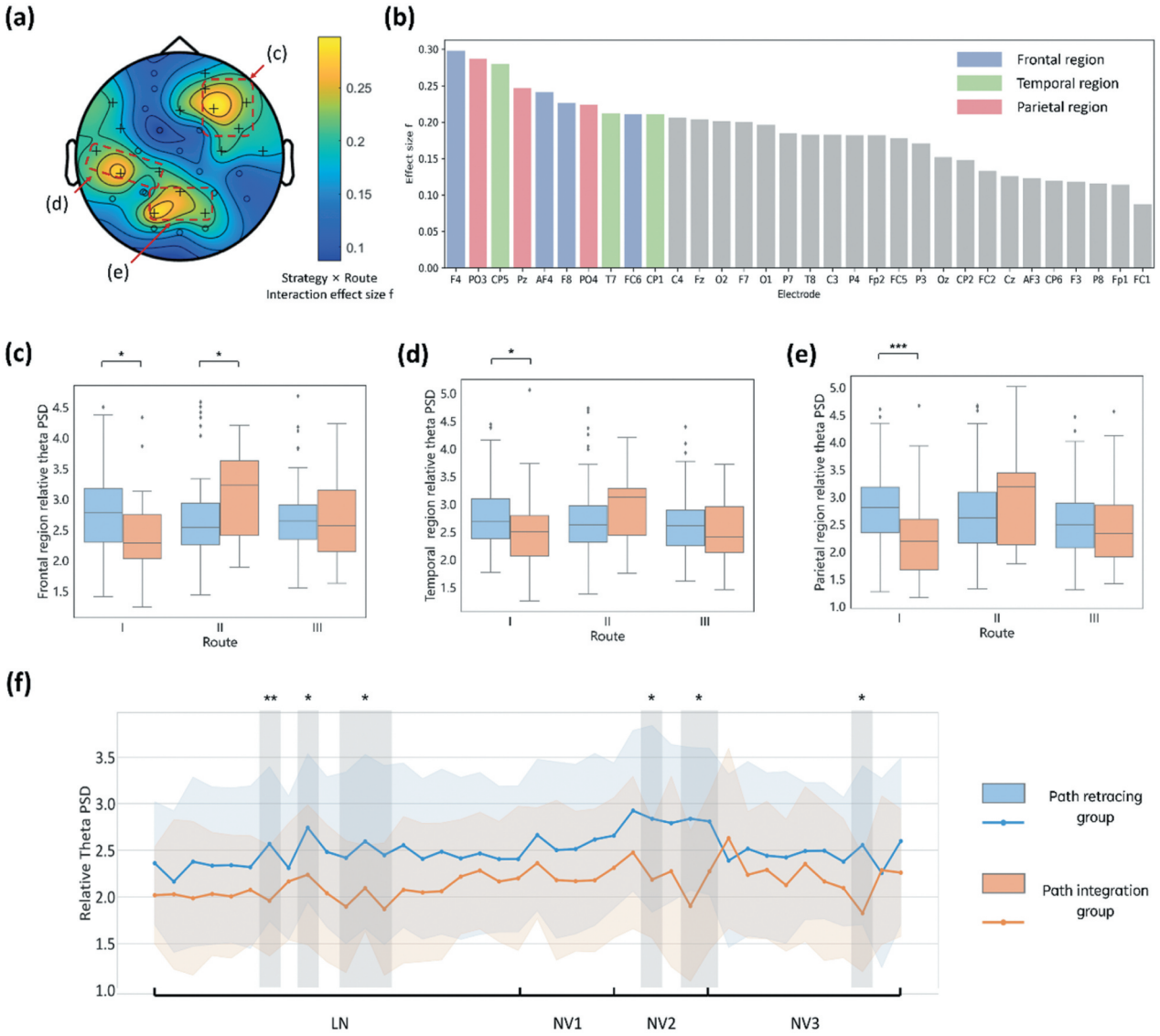

Figure 7. Relative theta PSD results. (a) The topomap of the strategy×route interaction effect is represented by effect size f values. (b) Effect size f value of each electrode. We clustered three regions of interest (ROIs), namely, frontal, temporal, and parietal regions, based on effect size and electrode adjacency relationship. (c)–(e) interaction effect plots depicting the relative theta PSD across different routes and strategies in the (c) frontal region (including F4, AF4, F8, and FC6); (d) temporal region (including T7, CP1, and CP5); and (e) parietal region (including Pz, PO3 and PO4). (f) The time series analysis results display the whole-brain relative theta PSD for route I. ("*" and "+" indicate $p < 0.05$, "**" indicates $p < 0.01$, "***" indicates $p < 0.001$, and the p-value is corrected by FDR.).

Finally, we identified correlations between the relative theta PSD and trajectory morphology. We observed a significant correlation between heading error and the frontal FC2 electrode ($r = 0.197$, $p < 0.05$, FDR-corrected).

5. Discussion

5.1. The differences between the two navigation strategies are manifested in the mastery of Euclidean space

In this study, we categorized participants into path retracing and path integration groups based on their decision-making differences in a virtual navigation environment. We then analyzed behavioral performance, scale scores, brain workload main effects, and interaction effects across different routes and task phases. At the behavioral level, our findings demonstrated the Hypothesis 1a and 1b: while the path integration was not the predominant strategy (Figure 3 (a) and Figure A1), it yielded superior performance in the NV task, with lower time costs and a shorter trajectory length (Figure 4). These results verified the effectiveness of shortcuts found by navigators in the path integration group in reducing the temporal and spatial costs of the NV task. Moreover, the SBSOD score showed that the performance of the NV task was related to the representation of Euclidean space, such as the sense of direction and distance (although not significant), and that the participants who used the path integration strategy had greater spatial ability. We validated the reliance of the path retracing group on known landmarks

Table 2. T-test results for three routes in three regions of interest.

Group			Descriptive			Inferential		
Route	ROI	Strategy	*N*	*M*	*SD*	*t*	*p*	*d*
I	Frontal	PR	53	2.795	0.726	2.536	0.013*	0.573
		PI	31	2.392	0.659			
	Temporal	PR	53	2.797	0.667	2.029	0.046*	0.459
		PI	31	2.486	0.697			
	Parietal	PR	53	2.819	0.772	3.429	0.001***	0.775
		PI	31	2.224	0.758			
II	Frontal	PR	64	2.630	0.737	−2.225	0.029*	−0.560
		PI	21	3.042	0.734			
	Temporal	PR	64	2.734	0.770	−1.155	0.251	−0.290
		PI	21	2.948	0.622			
	Parietal	PR	64	2.688	0.829	−1.054	0.295	−0.265
		PI	21	2.912	0.902			
III	Frontal	PR	59	2.712	0.602	0.583	0.562	0.132
		PI	29	2.627	0.707			
	Temporal	PR	59	2.644	0.598	1.368	0.175	0.310
		PI	29	2.456	0.623			
	Parietal	PR	59	2.551	0.696	0.447	0.656	0.101
		PI	29	2.476	0.806			

PR refers to path retracing strategy, PI refers to path integration strategy, *$p < 0.05$, **$p < 0.01$, ***$p < 0.001$.

and route knowledge, as evidenced by the alignment between the learned route in the LN task phase and the homing route. Additionally, we observed significantly greater pointing errors in the path retracing group, particularly in the PT1 and PT2 tasks – consistent with findings of He, Boone, and Hegarty (2023) and suggest an increase in pointing error with increasing distance to the destination, which is commonly attributed to cumulative errors in path integration (Cooper, Manka, and Mizumori 2001). This suggests that some participants, unable to mitigate integration errors in the virtual lunar terrain, defaulted to safer retracing strategies. These conclusions can be interpreted as a fusion of egocentric and allocentric reference frames during navigation (Burgess 2006; Ekstrom, Huffman, and Starrett 2017) while also suggesting a partial dissociation in human spatial references across different scales (Hegarty et al. 2006). Finally, the analysis of the trajectory morphology revealed that the path integration strategy group tended to navigate closer to their self-perceived destination, whereas the trajectory circuity and heading error of the path retracing group were significantly greater. Notably, owing to the medium effect size of the trajectory morphology results, further experiments are still needed to confirm the reliability of our results.

5.2. The cognitive load and brain workload of participants using the path integration strategy differ adaptively for routes with different levels of difficulty

Through feedback from the NASA-TLX scale, we discovered a strong positive correlation between the participants' time costs and self-reported cognitive load. Furthermore, exploratory analysis revealed that this subjective perception of cognitive load stemmed from negative feelings about task performance. Besides, we analyzed failed attempts (see Section "Exploratory analyses of failed trials" in the Appendix for details) and found that the participants in failed attempts reported that they felt more time pressure, whereas the participants using the path integration strategy felt less (Figure A2). In addition, the self-reported SBSOD scale results showed that the participants who believed that they had worse spatial ability tended to spend more time navigating home. Hence, we can infer that time pressure and a lack of spatial ability led to unconfident and negative emotions in task performance among navigators; thus, they tended to follow safer homing routes rather than taking risks to try shortcuts under time pressure. Although existing research has questioned the reliability and validity of self-reported scales (Boone, Gong, and Hegarty 2018), in this study, the SBSOD and the NASA-TLX scale were applied as supplements to the behavioral and cognitive data and provided new empirical evidence and explanations for how subjective cognitive load and emotions affect task performance (Chen et al. 2022; Galoyan et al. 2021Nakamura et al. 2022).

We found that the relative theta power was associated with "physical demand" components of the NASA-TLX scale. This suggests the relative theta power in this study may be correlated with the participants' physiological fatigue from sustained manual and visual tasks. Our results support Li and Chmiel (2024) that relative theta power is not entirely equivalent to cognitive load and may not always correlate with it. However, our findings indicate that relative theta power can serve to verify and supplement the cognitive dimensions assessed by subjective scales in cognitive experimental research. We also detected an interaction effect between strategy and route across multiple brain regions, including the ROIs in the frontal, temporal, and parietal regions. Among these ROIs, we observed that on route I, the theta power of

the path retracing group was greater than that of the path integration group, whereas the frontal theta power of the path integration group on route II was greater in contrast. Such findings were partially inconsistent with the Hypothesis 2. Previous studies have shown that the brain activities in the above regions are involved in memory (Blankenship et al. 2016; Jensen and Tesche 2002), visual information, and landmark knowledge processing (Cheng et al. 2023; Sulpizio et al. 2023). Therefore, we can infer that in specific routes, the brain workload of the navigators of the two strategies is reflected in the processing and memory of landmark cues. Considering the special navigation environment on the virtual lunar surface and the characteristics of different experimental routes, we try to explain this novel finding. This finding may be attributed to route II being the most extended and curved of the three routes; it imposed the greater theta power on participants in the path integration group and thus changed the difference between the two strategies. We can infer that in the virtual lunar surface, brain workload showed flexible adaptation among different routes when navigators used the path integration strategy, whereas no such adaptation was observed with the path retracing strategy. Different from the navigation research in the common virtual environments, the above conclusion does not prove a universal difference in brain workload between the two strategies. This may suggest that in our setups, path retracing in our paradigm necessitates active spatial awareness rather than mere habitual execution. Furthermore, both path retracing and path integration strategies appear to require complex spatial processing on the navigator's brain workload.

Through time series analysis, we observed that both strategies peaked in theta power during the mid-phase of the NV task at the whole-brain average level. This finding indicates that in the early phase of the NV task, there is a continuous accumulation of brain workload due to the construction of cognitive maps, whereas there is a reduction in the brain's demand for working memory as the participants approach the destination in the late phase. Finally, we also observed a correlation between the activation in the frontal, parietal, and occipital regions and between route circuity and heading error. This finding is consistent with the mental cost measured by a vector-based pedestrian navigation model (Bongiorno et al. 2021).

5.3. The distinctiveness of virtual lunar navigation

Although the study of path retracing versus path integration strategy is a classic research field, our study focused more on a unique virtual lunar navigation scenario that provided new empirical findings. Unlike virtual urban areas (Brunyé et al. 2012, 2017) and virtual maze scenes (He, Boone, and Hegarty 2023; Marchette, Bakker, and Shelton 2011), the unstructured nature of the lunar surface impedes navigators from constructing cognitive maps based on road network information. In contrast, navigators find it easier to infer locations through the learned positional relationships between landmarks and trajectories. As a result, this study revealed that navigators' choice of path integration strategy was inhibited. Besides, in natural virtual environments, lunar scenes also differ from the Earth's forest and desert scenes (Foo et al. 2005). The unique landscape features of the lunar surface, such as impact craters, gravel, and the sky, are quite different from the familiar landscapes on Earth. Even if a desert scene has terrain similar to that of a lunar surface scene, the characteristics of the lunar surface and the maneuverability of the virtual lunar rover may be unfamiliar to the navigator, increasing the difficulty of adapting to the navigation environment on the lunar surface. The analysis results suggested that the lunar landscape without navigational aids likely contributed to a heightened mental burden and excessive cognitive processing, particularly for participants with limited spatial ability. Notably, the behavior and cognitive status of participants in large-scale high ecological validity scenes can better represent real-world performance than those in cases with highly controlled experimental scenes (Dong et al. 2022). Although previous studies have examined human cognitive processes during navigation through rigorous control variable experimental paradigms, we have demonstrated that these cognitive processes are not entirely consistent in virtual lunar scenes.

5.4. Limitations and future work

In this study, we classified participants dichotomously into path retracing and path integration groups, yet did not yet did not address potential hybrid combinations or dynamic transitions between these strategies – avenues warranting exploration in subsequent studies. Such explorations could entail assessing neural circuit activations (e.g. the "what" and "where" pathways) through a controlled paradigm employing fMRI techniques. In future research, deeper insights by integrating advanced EEG analyses with participant interviews to enhance our understanding of navigators' decision-making processes and emotional responses, and to achieve more reliable cross-validation.

Furthermore, the experimental design could enhance immersion by using VR devices and dynamic landmark cues to encourage participants to make decisions that are more correlated with the real scene. The experimental design could also involve an unknown Earth environment without navigation aids, thereby examining whether performance and cognitive differences exist in similar challenging setups.

Finally, this study detected no demographic differences across the two strategy groups; consequently, such metrics were deprioritized in analyses. With respect to existing studies (Dabbs et al. 1998; Kühn et al. 2014; Wiener et al. 2013), future efforts should consider the influences of gender, age, and video gaming expertise on navigation performance in virtual lunar scenes.

6. Conclusions

Previous studies have compared the behavioral and cognitive processes of path retracing and path integration strategies. However, few studies have investigated these two strategies within virtual lunar surface simulations characterized by high ecological validity. In this study, a novel virtual lunar surface exploration scene was developed to analyze navigators' performance and brain workload across spatial learning, navigation, and destination-pointing tasks. Based on the behavioral, scale, and EEG data, our findings confirmed better performance for the path integration strategy. In addition, the path integration strategy was found to allow for dynamic modulation of cognitive resources in response to the navigation scene complexity, enabling navigators to better adapt to diverse navigation scenarios. Our primary contribution lies in providing empirical evidence for the navigation behaviors and cognitive mechanisms of path retracing and path integration strategies in virtual lunar scenes, which will not only facilitate the training of lunar exploration personnel but also help in the development of intelligent, adaptive navigation systems for forthcoming space missions.

Disclosure statement

No potential conflict of interest was reported by the author(s).

Funding

This work was supported by the National Natural Science Foundation of China (NSFC) [Grant No. 42230103].

Notes on contributors

Bowen Shi is currently a PhD student in Urban Informatics and Smart City at The Hong Kong Polytechnic University, Hong Kong, China. His research interests are geospatial cognition, brain-like intelligent navigation and mobility science.

Tong Qin is currently a PhD student in the Cartography and GIS Research Group, Department of Geography, Ghent University, Belgium. His research interests include map usability, spatial cognition, and urban perception using neuroscientific techniques.

Bing He is currently a PhD student in Geographic Information Science and Remote Sensing at Beijing Normal University, China. His research focuses on intelligent interpretation of remote sensing data, spatial cognition, and cognitive computational science.

Lingli Mu received the PhD degree in Cartography and GIS from the University of Chinese Academy of Sciences. He is currently a Professor of Technology and Engineering Center for Space Utilization at the Chinese Academy of Sciences, China. His research focuses on lunar mapping, AI for lunar exploration, and planetary remote sensing.

Weihua Dong received the PhD degree in Cartography and Geographic Information Engineering from Wuhan University. He is currently a Professor of the Faculty of Geographical Science at Beijing Normal University and the director of the Research Center for Geospatial Cognition and Visual Analysis of Beijing Normal University. He regularly serves as an Editorial member for Cartography and Geographic Information Science, Journal of Location Based Services, and as a Guest Editor for ISPRS International Journal of Geo-Information. He is also a member of the Cognitive Working Committee of the International Cartographic Association (ICA). His research focuses on geospatial cognition and brain-like intelligent navigation.

ORCID

Bowen Shi http://orcid.org/0000-0002-4753-7572
T. Qin http://orcid.org/0000-0001-5724-2105
B. He http://orcid.org/0000-0003-3012-0348
W. Dong http://orcid.org/0000-0001-6097-7946

Data and codes availability statement

The data that support the findings of this study are openly available in OSF at http://doi.org/10.17605/OSF.IO/EZ387.

References

Anggraini, D., S. Glasauer, and K. Wunderlich. 2018. "Neural Signatures of Reinforcement Learning Correlate with Strategy Adoption During Spatial Navigation." *Scientific Reports* 8 (1): 10110. https://doi.org/10.1038/s41598-018-28241-z.

Ballou, R. H., H. Rahardja, and N. Sakai. 2002. "Selected Country Circuity Factors for Road Travel Distance Estimation." *Transportation Research Part A: Policy and Practice* 36 (9): 843–848. https://doi.org/10.1016/s0965-8564(01)00044-1.

Barhorst-Cates, E. M., K. M. Rand, and S. H. Creem-Regehr. 2016. "The Effects of Restricted Peripheral Field-of-View on Spatial Learning While Navigating." *PLOS ONE* 11 (10): e0163785. https://doi.org/10.1371/journal.pone.0163785.

Bian, Z., Q. Li, L. Wang, C. Lu, S. Yin, and X. Li. 2014. "Relative Power and Coherence of EEG Series are Related to Amnestic Mild Cognitive Impairment in Diabetes." *Frontiers in Aging Neuroscience* 6:11. https://doi.org/10.3389/fnagi.2014.00011.

Blankenship,T.L., M.O'Neill, K.Deater-Deckard, R.A.Diana, and M.A.Bell. 2016. "Frontotemporal Functional Connectivity and Executive Functions Contribute to Episodic Memory Performance." *International Journal of Psychophysiology* 107:72–82. https://doi.org/10.1016/j.ijpsycho.2016.06.014.

Bohbot, V., S. McKenzie, K. Konishi, C. Fouquet, V. Kurdi, R. Schachar, M. Boivin, and P. Robaey. 2012. "Virtual Navigation Strategies from Childhood to Senescence: Evidence for Changes Across the Life Span." *Frontiers in Aging Neuroscience* 4:28. https://doi.org/10.3389/fnagi.2012.00028.

Bongiorno, C., Y. Zhou, M. Kryven, D. Theurel, A. Rizzo, P. Santi, J. Tenenbaum, and C. Ratti. 2021. "Vector-Based Pedestrian Navigation in Cities." *Nature Computational Science* 1 (10): 678–685. https://doi.org/10.1038/s43588-021-00130-y.

Boone, A. P., X. Gong, and M. Hegarty. 2018. "Sex Differences in Navigation Strategy and Efficiency." *Memory & Cognition* 46 (6): 909–922. https://doi.org/10.3758/s13421-018-0811-y.

Brunyé, T. T., A. Gardony, C. R. Mahoney, and H. A. Taylor. 2012. "Going to Town: Visualized Perspectives and Navigation Through Virtual Environments." *Computers in Human Behavior* 28 (1): 257–266. https://doi.org/10.1016/j.chb.2011.09.008.

Brunyé, T. T., M. D. Wood, L. A. Houck, and H. A. Taylor. 2017. "The Path More Travelled: Time Pressure Increases Reliance on Familiar Route-Based Strategies During Navigation." *Quarterly Journal of Experimental Psychology* 70 (8): 1439–1452. https://doi.org/10.1080/17470218.2016.1187637.

Burgess, N. 2006. "Spatial Memory: How Egocentric and Allocentric Combine." *Trends in Cognitive Sciences* 10 (12): 551–557. https://doi.org/10.1016/j.tics.2006.10.005.

Caplan, J. B., J. R. Madsen, A. Schulze-Bonhage, R. Aschenbrenner-Scheibe, E. L. Newman, and M. J. J. T. J. Kahana. 2003. "Human θ Oscillations Related to Sensorimotor Integration and Spatial Learning." *Journal of Neuroscience* 23 (11): 4726–4736. https://doi.org/10.1523/JNEUROSCI.23-11-04726.2003.

Cavanagh, J. F., and M. J. Frank. 2014. "Frontal Theta as a Mechanism for Cognitive Control." *Trends in Cognitive Sciences* 18 (8): 414–421. https://doi.org/10.1016/j.tics.2014.04.012.

Chen,Y.H., C. Z. Yang, Y. Gu, and B. Y. Hu. 2022. "Influence of Mobile Robots on Human Safety Perception and System Productivity in Wholesale and Retail Trade Environments: APilot Study." *IEEE Transactions on Human-Machine Systems* 52(4): 624–635. https://doi.org/10.1109/thms.2021.3134553.

Cheng, B. J., E. R. Lin, A. Wunderlich, K. Gramann, and S. I. Fabrikant. 2023. "Using Spontaneous Eye Blink-Related Brain Activity to Investigate Cognitive Load During Mobile Map-Assisted Navigation." *Frontiers in Neuroscience* 17:17. https://doi.org/10.3389/fnins.2023.1024583.

Cheng, B. J., A. Wunderlich, K. Gramann, E. R. Lin, and S. I. Fabrikant. 2022. "The Effect of Landmark Visualization in Mobile Maps on Brain Activity During Navigation: A Virtual Reality Study." *Frontiers in Virtual Reality* 3:3. https://doi.org/10.3389/frvir.2022.981625.

Chersi, F., and N. Burgess. 2015. "The Cognitive Architecture of Spatial Navigation: Hippocampal and Striatal Contributions." *Neuron* 88 (1): 64–77. https://doi.org/10.1016/j.neuron.2015.09.021.

Chrastil,E.R., C.Rice, M.Goncalves, K.N.Moore, S.C.Wynn, C. E.Stern, and E.Nyhus. 2022. "Theta Oscillations Support Active Exploration in Human Spatial Navigation." *Neuroimage* 262:119581. https://doi.org/10.1016/j.neuroimage.2022.119581.

Christensen, S. C., and H. H. Wright. 2014. "Quantifying the Effort Individuals with Aphasia Invest in Working Memory Tasks Through Heart Rate Variability." *American Journal of Speech-Language Pathology* 23 (2): 361–371. https://doi.org/10.1044/2014_ajslp-13-0082.

Condappa, O., and J. M. Wiener. 2014. "Human Place and Response Learning: Navigation Strategy Selection, Pupil Size and Gaze Behavior." *Psychological Research* 80 (1): 82–93. https://doi.org/10.1007/s00426-014-0642-9.

Cooper, B. G., T. F. Manka, and S. J. Mizumori. 2001. "Finding Your Way in the Dark: The Retrosplenial Cortex Contributes to Spatial Memory and Navigation without Visual Cues." *Behavioral Neuroscience* 115 (5): 1012–1028. https://doi.org/10.1037/0735-7044.115.5.1012.

Cornwell,B.R., L.L.Johnson, T.Holroyd, F.W.Carver, and C. Grillon. 2008. "Human Hippocampal and Parahippocampal Theta During Goal-Directed Spatial Navigation Predicts Performance on aVirtual Morris Water Maze." *Journal of Neuroscience* 28(23): 5983–5990. https://doi.org/10.1523/jneurosci.5001-07.2008.

Dabbs,J.M., E.L.Chang, R. A. Strong, and R. Milun. 1998. "Spatial Ability, Navigation Strategy, and Geographic Knowledge Among Men and Women." *Evolution and Human Behavior* 19 (2): 89–98. https://doi.org/10.1016/s1090-5138(97)00107-4.

Delorme,A., and S.Makeig. 2004. "EEGLAB: An Open Source Toolbox for Analysis of Single-Trial EEG Dynamics Including Independent Component Analysis." *Journal of Neuroscience Methods* 134(1): 9–21. https://doi.org/10.1016/j.jneumeth.2003.10.009.

Dong, W., T. Qin, T. Yang, H. Liao, B. Liu, L. Meng, and Y. Liu. 2022. "Wayfinding Behavior and Spatial Knowledge Acquisition: Are They the Same in Virtual Reality and in real-World Environments?" *Annals of the American Association of Geographers* 112 (1): 226–246. https://doi.org/10.1080/24694452.2021.1894088.

Ekstrom,A.D., A.E.G.F.Arnold, and G.Iaria. 2014. "ACritical Review of the Allocentric Spatial Representation and Its Neural Underpinnings: Toward a Network-Based Perspective." *Frontiers in Human Neuroscience* 8. https://doi.org/10.3389/fnhum.2014.00803.

Ekstrom, A. D., D. J. Huffman, and M. Starrett. 2017. "Interacting Networks of Brain Regions Underlie Human Spatial Navigation: A Review and Novel Synthesis of the Literature." *Journal of Neurophysiology* 118 (6): 3328–3344. https://doi.org/10.1152/jn.00531.2017.

Fabroyir, H., and W.-C. Teng. 2018. "Navigation in Virtual Environments Using Head-Mounted Displays: Allocentric Vs. Egocentric Behaviors." *Computers in Human Behavior* 80:331–343. https://doi.org/10.1016/j.chb.2017.11.033.

Foo, P., W. Warren, A. Duchon, and M. Tarr. 2005. "Do Humans Integrate Routes into a Cognitive Map? Map- Versus Lndmark-Based Navigation of Novel Shortcuts." *Journal of Experimental Psychology: Learning, Memory & Cognition* 31 (2): 195–215. https://doi.org/10.1037/0278-7393.31.2.195.

Galoyan, T., K. Betts, H. Abramian, P. Reddy, K. Izzetoglu, and P. A. Shewokis. 2021. "Examining Mental Workload in a Spatial Navigation Transfer Game via Functional Near Infrared Spectroscopy." *Brain Sciences* 11 (1): 45. https://doi.org/10.3390/brainsci11010045.

Gardner, R. S., D. F. Suarez, N. K. Robinson-Burton, C. J. Rudnicky, A. Gulati, G. A. Ascoli, and T. C. Dumas. 2016. "Differential Arc Expression in the Hippocampus and Striatum During the Transition from Attentive to Automatic Navigation on a Plus Maze."

Neurobiology of Learning and Memory 131:36–45. https://doi.org/10.1016/j.nlm.2016.03.008.

Gevins, A., and M. E. Smith. 2000. "Neurophysiological Measures of Working Memory and Individual Differences in Cognitive Ability and Cognitive Style." *Cerebral Cortex* 10 (9): 829–839. https://doi.org/10.1093/cercor/10.9.829.

Goodroe, S. C., and H. J. Spiers. 2022. "Extending Neural Systems for Navigation to Hunting Behavior." *Current Opinion in Neurobiology* 73:102545. https://doi.org/10.1016/j.conb.2022.102545.

Gramann,K., J.Onton, D.Riccobon, H.J.Mueller, S.Bardins, and S.Makeig. 2010. "Human Brain Dynamics Accompanying Use of Egocentric and Allocentric Reference Frames During Navigation." *Journal of Cognitive Neuroscience* 22(12): 2836–2849. https://doi.org/10.1162/jocn.2009.21369.

Gramfort,A., M.Luessi, E.Larson, D.A.Engemann, D. Strohmeier, C.Brodbeck, R.Goj, etal. 2013. "MEG and EEG Data Analysis with MNE-Python." *Frontiers in Neuroscience* 7:267. https://doi.org/10.3389/fnins.2013.00267.

Hafting, T., M. Fyhn, S. Molden, M.-B. Moser, and E. I. Moser. 2005. "Microstructure of a Spatial Map in the Entorhinal Cortex." *Nature* 436 (7052): 801–806. https://doi.org/10.1038/nature03721.

Hart, S. G., and L. E. Staveland. 1988. *Advances in Psychology*. Edited by Peter A. Hancock and Najmedin Meshkati Vol. 52. Netherlands: North-Holland.

He, C., A. P. Boone, and M. Hegarty. 2023. "Measuring Configural Spatial Knowledge: Individual Differences in Correlations Between Pointing and Shortcutting." *Psychonomic Bulletin & Review* 30 (5): 1802–1813. https://doi.org/10.3758/s13423-023-02266-6.

Hegarty, M., C. He, A. Boone, S. Yu, E. Jacobs, and E. Chrastil. 2022. "Understanding Differences in Wayfinding Strategies." *Topics in Cognitive Science* 15 (1): 15. https://doi.org/10.1111/tops.12592.

Hegarty,M., D.R.Montello, A.E.Richardson, T.Ishikawa, and K.Lovelace. 2006. "Spatial Abilities at Different Scales: Individual Differences in Aptitude-Test Performance and Spatial-Layout Learning." *Intelligence* 34(2): 151–176. https://doi.org/10.1016/j.intell.2005.09.005.

Hegarty, M., A. E. Richardson, D. R. Montello, K. Lovelace, and I. Subbiah. 2002. "Development of a Self-Report Measure of Environmental Spatial Ability." *Intelligence* 30 (5): 425–447. https://doi.org/10.1016/s0160-2896(02)00116-2.

IBM. 2019. *IBM SPSS Statistics for Windows*. USA: IBM Corp.

Jensen, O., and C. D. Tesche. 2002. "Frontal Theta Activity in Humans Increases with Memory Load in a Working Memory Task." *European Journal of Neuroscience* 15 (8): 1395–1399. https://doi.org/10.1046/j.1460-9568.2002.01975.x.

Kahana, M. J., D. Seelig, and J. R. Madsen. 2001. "Theta returns." *Current Opinion in Neurobiology* 11 (6): 739–744. https://doi.org/10.1016/S0959-4388(01)00278-1.

Kosch, T., M. Hassib, D. Buschek, and A. Schmidt. 2018. "Look into My Eyes: Using Pupil Dilation to Estimate Mental Workload for Task Complexity Adaptation." Paper presented at the CHI Conference on Human Factors in Computing Systems (CHI), Montreal, Canada, Apr 21-26.

Kühn, S., T. Gleich, R. C. Lorenz, U. Lindenberger, and J. Gallinat. 2014. "Playing Super Mario Induces Structural Brain Plasticity: Gray Matter Changes Resulting from Training with a Commercial Video Game." *Molecular Psychiatry* 19 (2): 265–271. https://doi.org/10.1038/mp.2013.120.

Lawton, C. A. 1994. "Gender Differences in Way-Finding Strategies: Relationship to Spatial Ability and Spatial Anxiety." *Sex Roles* 30 (11): 765–779. https://doi.org/10.1007/bf01544230.

Lenhard, W., and A. Lenhard. 2022. *Computation of Effect Sizes*. Germany: Psychometrica. https://www.psychometrica.de/effect_size.html.

Li, T., and A. Chmiel. 2024. "Automatic Subtitles Increase Accuracy and Decrease Cognitive Load in Simultaneous Interpreting." *Interpreting* 26 (2): 253–281. https://doi.org/10.1075/intp.00111.li.

Liu, J., A. K. Singh, and C. T. Lin. 2022. "Predicting the Quality of Spatial Learning via Virtual Global Landmarks." *IEEE Transactions on Neural Systems and Rehabilitation Engineering* 30:2418–2425. https://doi.org/10.1109/tnsre.2022.3199713.

Maier, P. M., D. Iggena, C. J. Ploner, and C. Finke. 2024. "Memory Consolidation Affects the Interplay of Place and Response Navigation." *Cortex* 175:12–27. https://doi.org/10.1016/j.cortex.2024.04.002.

Marchette, S., A. Bakker, and A. Shelton. 2011. "Cognitive Mappers to Creatures of Habit: Differential Engagement of Place and Response Learning Mechanisms Predicts Human Navigational Behavior." *Journal of Neuroscience* 31 (43): 15264–15268. https://doi.org/10.1523/jneurosci.3634-11.2011.

Miyakoshi, M., L. Gehrke, K. Gramann, S. Makeig, J. Iversen, and M. Seeber. 2021. "The Audiomaze: An EEG and Motion Capture Study of Human Spatial Navigation in Sparse Augmented Reality." *European Journal of Neuroscience* 54 (12): 8283–8307. https://doi.org/10.1111/ejn.15131.

Nakamura, F., A. Verhulst, K. Sakurada, M. Fukuoka, and M. Sugimoto. 2022. "Evaluation of Spatial Directional Guidance Using Cheek Haptic Stimulation in a Virtual Environment." *Frontiers in Computer Science* 4:733844. https://doi.org/10.3389/fcomp.2022.733844.

Nourbakhsh, N., Y. Wang, and F. Chen. 2013. "GSR and Blink Features for Cognitive Load Classification." Paper presented at the 14th IFIP TC 13 INTERACT International Conference on Designing for Diversit, Cape Town, South Africa, Sep 02-06.

O'Keefe, J., and J. Dostrovsky. 1971. "The Hippocampus as a Spatial Map. Preliminary Evidence from Unit Activity in the Freely-Moving Rat." *Brain Research* 34 (1): 171–175. https://doi.org/10.1016/0006-8993(71)90358-1.

Oostenveld, R., P. Fries, E. Maris, and J.-M. Schoffelen. 2011. "FieldTrip: Open Source Software for Advanced Analysis of MEG, EEG, and Invasive Electrophysiological Data." *Computational Intelligence and Neuroscience* 1:1–9. https://doi.org/10.1155/2011/156869.

Paas, F., J. E. Tuovinen, H. Tabbers, and P. W. M. Van Gerven. 2003. "Cognitive Load Measurement as a Means to Advance Cognitive Load Theory." *Educational Psychologist* 38 (1): 63–71. https://doi.org/10.1207/S15326985EP3801_8.

Paas, F., and J. J. G. Van Merrienboer. 1993. "The Efficiency of Instructional Conditions: An Approach to Combine Mental Effort and Performance Measures." *Human Factors: The Journal of the Human Factors & Ergonomics Society* 35 (4): 737–743. https://doi.org/10.1177/001872089303500412.

Packard, M. G., and J. L. McGaugh. 1996. "Inactivation of Hippocampus or Caudate Nucleus with Lidocaine

Differentially Affects Expression of Place and Response Learning." *Neurobiology of Learning and Memory* 65 (1): 65–72. https://doi.org/10.1006/nlme.1996.0007.

Plank, M., J. Snider, E. Kaestner, E. Halgren, and H. Poizner. 2015. "Neurocognitive Stages of Spatial Cognitive Mapping Measured During Free Exploration of a Large-Scale Virtual Environment." *Journal of Neurophysiology* 113 (3): 740–753. https://doi.org/10.1152/jn.00114.2014.

Reid, G. B., and T. E. Nygren Peter A. Hancock and Najmedin Meshkati, Edited by. 1988. *Advances in Psychology*. Vol. 52. Netherlands: North-Holland.

Riecke, B., H.-J. Veen, and H. Bülthoff. 2002. "Visual Homing is Possible without Landmarks – A Path Integration Study in Virtual Reality." *Presence* 11 (5): 443–473. https://doi.org/10.1162/105474602320935810.

Saitis, C., and K. Kalimeri. 2016. "Identifying Urban Mobility Challenges for the Visually Impaired with Mobile Monitoring of Multimodal Biosignals." Paper presented at the Universal Access in Human-Computer Interaction. Users and Context Diversity, Cham.

Santos-Pata, D., and P. Verschure. 2018. "Human Vicarious Trial and Error is Predictive of Spatial Navigation Performance." *Frontiers in Behavioral Neuroscience* 12:12. https://doi.org/10.3389/fnbeh.2018.00237.

Schug, M. G. 2016. "Geographical Cues and Developmental Exposure: Navigational Style, Wayfinding Anxiety, and Childhood Experience in the Faroe Islands." *Human Nature* 27 (1): 68–81. https://doi.org/10.1007/s12110-015-9245-4.

Siegel, A. W., and S. H. White. 1975. "The Development of Spatial Representations of Large-Scale Environments." *Advances in Child Development and Behavior* 10:9–55. https://doi.org/10.1016/S0065-2407(08)60007-5.

Smith, A. D., L. McKeith, and C. J. Howard. 2013. "The Development of Path Integration: Combining Estimations of Distance and Heading." *Experimental Brain Research* 231 (4): 445–455. https://doi.org/10.1007/s00221-013-3709-8.

Steck, S. D., and H. A. Mallot. 2000. "The Role of Global and Local Landmarks in Virtual Environment Navigation." *Presence Teleoperators & Virtual Environments* 9 (1): 69–83. https://doi.org/10.1162/105474600566628.

Sulpizio, V., P. Fattori, S. Pitzalis, and C. Galletti. 2023. "Functional Organization of the Caudal Part of the Human Superior Parietal Lobule." *Neuroscience and Biobehavioral Reviews* 153:105357. https://doi.org/10.1016/j.neubiorev.2023.105357.

Taillade, M., B. N'Kaoua, and H. Sauzéon. 2016. "Age-Related Differences and Cognitive Correlates of Self-Reported and Direct Navigation Performance: The Effect of Real and Virtual Test Conditions Manipulation." *Frontiers in Psychology* 6:6. https://doi.org/10.3389/fpsyg.2015.02034.

Taube, J. S., R. U. Muller, and J. B. Ranck. 1990. "Head-Direction Cells Recorded from the Postsubiculum in Freely Moving Rats. I. Description and Quantitative Analysis." *Journal of Neuroscience* 10 (2): 420–435. https://doi.org/10.1523/jneurosci.10-02-00420.1990.

Teixeira De Almeida, M., M. Seeber, K. Gschwend, R. Maurer, I. Faulmann, and N. Burra. 2023. "Electrophysiological Correlates of Distance and Direction Processing During Cognitive Map Retrieval: A Source Analysis." *Frontiers in Human Neuroscience* 17:1062064. https://doi.org/10.3389/fnhum.2023.1062064.

Tolman, E. C. 1948. "Cognitive Maps in Rats and Men." *Psychological Review* 55 (4): 189–208. https://doi.org/10.1037/h0061626.

Vigário, R. N. 1997. "Extraction of Ocular Artefacts from EEG Using Independent Component Analysis." *Electroencephalography and Clinical Neurophysiology* 103 (3): 395–404. https://doi.org/10.1016/s0013-4694(97)00042-8.

Weidemann, C. T., M. V. Mollison, and M. J. Kahana. 2009. "Electrophysiological Correlates of High-Level Perception During Spatial Navigation." *Psychonomic Bulletin & Review* 16 (2): 313–319. https://doi.org/10.3758/pbr.16.2.313.

Wiener, J. M., O. Condappa, M. A. Harris, and T. Wolbers. 2013. "Maladaptive Bias for Extrahippocampal Navigation Strategies in Aging Humans." *Journal of Neuroscience* 33 (14): 6012–6017. https://doi.org/10.1523/jneurosci.0717-12.2013.

Wiener, J. M., H. Kmecova, and O. Condappa. 2012. "Route Repetition and Route Retracing: Effects of Cognitive Aging." *Frontiers in Aging Neuroscience* 4:7. https://doi.org/10.3389/fnagi.2012.00007.

Yang, X., E. McCoy, E. Anaya-Boig, I. Avila-Palencia, C. Brand, G. Carrasco-Turigas, E. Dons, et al. 2021. "The Effects of Traveling in Different Transport Modes on Galvanic Skin Response (GSR) as a Measure of Stress: An Observational Study." *Environment International* 156:106764. https://doi.org/10.1016/j.envint.2021.106764.

Yang, X. N., and J. H. Kim. 2019. "Measuring Workload in a Multitasking Environment Using Fractal Dimension of Pupil Dilation." *International Journal of human–Computer Interaction* 35 (15): 1352–1361. https://doi.org/10.1080/10447318.2018.1525022.

Yesiltepe, D., R. Conroy Dalton, and A. Ozbil Torun. 2021. "Landmarks in Wayfinding: A Review of the Existing Literature." *Cognitive Processing* 22 (3): 369–410. https://doi.org/10.1007/s10339-021-01012-x.

Zhao, M., and W. H. Warren. 2015. "Environmental Stability Modulates the Role of Path Integration in Human Navigation." *Cognition* 142:96–109. https://doi.org/10.1016/j.cognition.2015.05.008.

Zheng, B., X. T. Jiang, G. Tien, A. Meneghetti, O. N. M. Panton, and M. S. Atkins. 2012. "Workload Assessment of Surgeons: Correlation Between NASA TLX and Blinks." *Surgical Endoscopy and Other Interventional Techniques* 26 (10): 2746–2750. https://doi.org/10.1007/s00464-012-2268-6.

Appendices

Appendix A. Exploratory analyses of failed trials

In this study, we focused on navigation process differences between participants using path retracing and path integration strategies. We excluded 36 samples where participants failed to return to the lunar base from the main analysis since we could not subjectively assign failed trajectories to either strategy group. In this section, we conducted exploratory analyses to investigate navigational decision-making and self-reported cognitive load in these failure cases.

In Figure A1, we first illustrate the homing trajectories of failed cases. By comparing these failed attempts with the learned routes, we observed that most failed trajectories initially align closely with the learned routes but become more scattered in later sections. Notably, only in route I and route II did we see one trajectory each that appears to attempt a shortcut, a pattern absents in route III. We hypothesized that this difference may be due to participants in failed attempts initially relying on a path retracing strategy. However, accumulated errors and limited landmark cues likely led to disorientation and failure outcomes.

We also explored the self-reported NASA-TLX scores of the failed trials. Thus, we performed a one-way ANOVA for the NASA-TLX score on different groups (due to the participant's misunderstanding of the scale, 2 trials from the path retracing group, 1 trial from the path integration group, and 2 trials from the failed group were removed from this analysis). The ANOVA results for the NASA-TLX score revealed a significant effect on subject workload between the path retracing, path integration, and failed trial groups ($F(2,116) = 35.663$, $p < 0.001$, FDR-corrected; $f = 0.835$). We further examined the post-hoc T-test results for the six workload dimensions and found that the "temporal demand" dimension significantly differed between the path retracing and path integration groups ($t(83) = 2.473$, $p < 0.05$), the path retracing and failed groups ($t(90) = -3.480$, $p < 0.05$), and the path integration and failed groups ($t(59) = -5.433$, $p < 0.001$) (Figure A2).

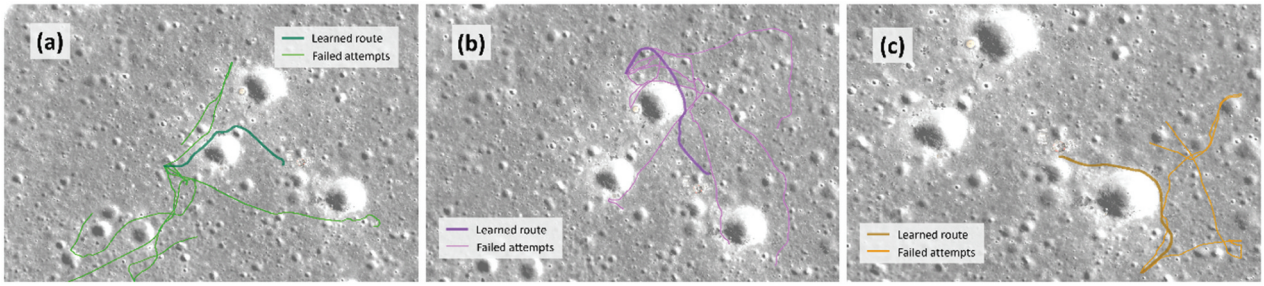

Figure A1. Trajectories of the failed attempts on (a) route I, (b) route II, (c) route III.

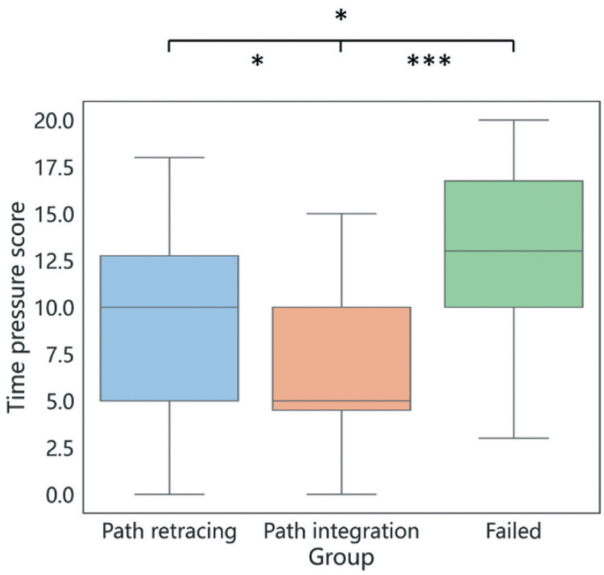

Figure A2. Time pressure scale score between different strategies and failed trials (*$p < 0.05$, **$p < 0.01$, ***$p < 0.001$, FDR-corrected).

Appendix B. Summary figures and tables of detailed statistical data

In this section, we report the statistical data, including post-hoc T-tests results for the behavioral metrics, correlations between each scale score and time costs, between relative theta power and NASA-TLX scores, and the interaction effect of strategy×route for each EEG electrode. For brevity, these data are not presented in the main text.

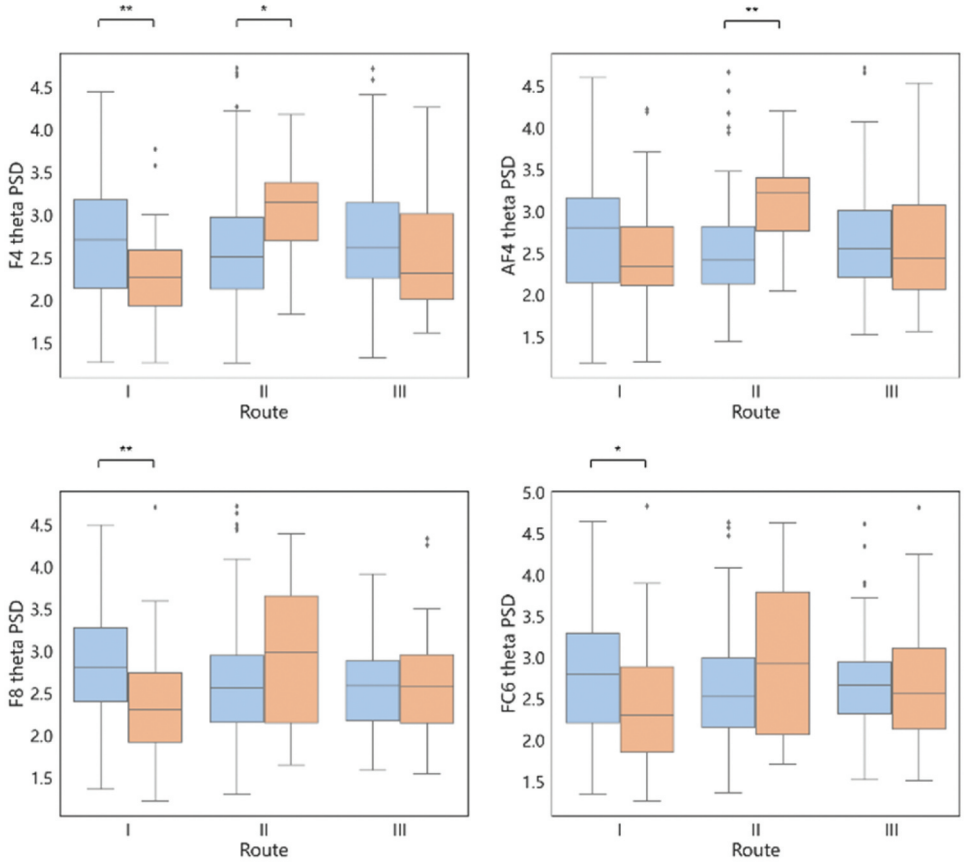

Figure A3. Interaction effect plots depicting the relative theta PSD across different routes and strategies in the frontal region (F4, AF4, F8, and FC6 included. The blue boxes represent the path retracing group, and the orange boxes represent the path integration group. *$p < 0.05$, **$p < 0.01$, FDR-corrected).

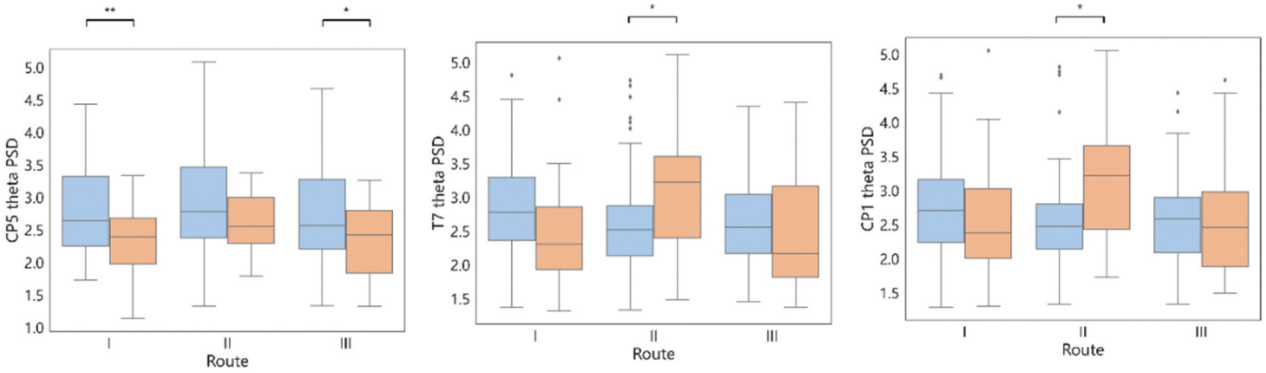

Figure A4. Interaction effect plots depicting the relative theta PSD across different routes and strategies in the temporal region (CP1, T7, and CP5 included. The blue boxes represent the path retracing group, and the orange boxes represent the path integration group. *$p < 0.05$, **$p < 0.01$, FDR-corrected).

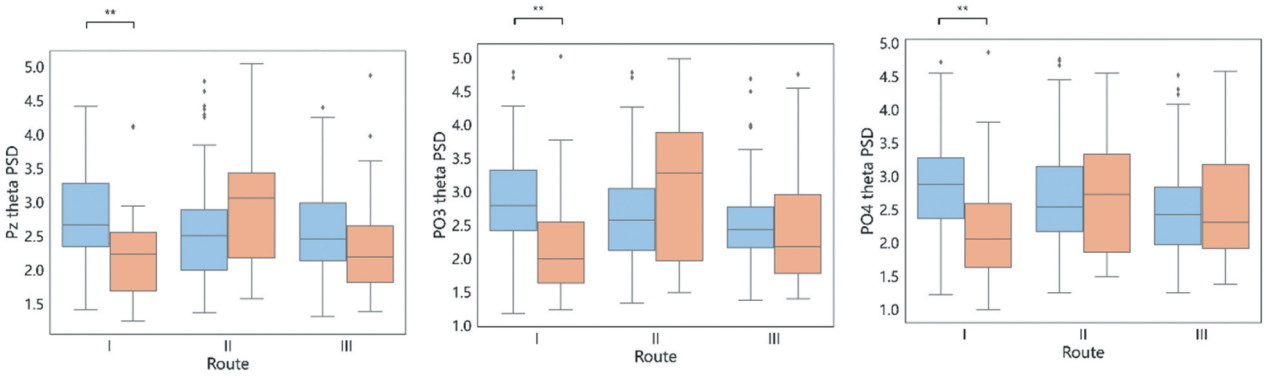

Figure A5. Interaction effect plots depicting the relative theta PSD across different routes and strategies in the parietal region (pz, PO3 and PO4 included. The blue boxes represent the path retracing group, and the orange boxes represent the path integration group. $^{**}p < 0.01$, FDR-corrected).

Table A1. T-test results of behavioral metrics between two strategy groups across different conditions ($^{*}p < 0.05$, $^{**}p < 0.01$, $^{***}p < 0.001$).

		Descriptive						Inferential		
		Path retracing strategy			Path integration strategy			T-test		Effect size
Metric	Condition	*N*	*M*	*SD*	*N*	*M*	*SD*	*t*	*p*	Cohen's d
Time cost (TC)	All routes	60	280.12	48.90	28	224.63	39.67	5.248	0.000***	1.201
	Route I	18	269.89	35.64	11	243.20	45.81	1.757	0.090	0.672
	Route II	22	298.42	51.86	7	218.13	25.67	3.911	0.001***	1.697
	Route III	20	269.20	52.01	10	208.74	34.88	3.308	0.003**	1.281
Trajectory length (TL)	All routes	60	1949.73	285.87	28	1526.55	159.70	7.305	0.000***	1.672
	Route I	18	1879.16	114.64	11	1641.16	137.46	5.032	0.000***	1.926
	Route II	22	2119.11	300.92	7	1569.05	67.78	4.742	0.000***	2.058
	Route III	20	1826.93	296.83	10	1370.74	89.54	4.717	0.000***	1.827
Pointing error (PE)	All phases	178	27.97	25.84	84	16.53	11.90	3.868	0.000***	0.512
	PT1	58	37.51	33.50	28	15.19	10.74	3.433	0.001***	0.790
	PT2	60	24.46	22.15	28	13.90	9.89	2.407	0.018*	0.551
	PT3	60	22.26	17.12	28	20.49	14.03	0.478	0.634	0.109
Heading error (HE)	All phases	178	24.14	19.00	84	17.86	13.94	2.703	0.007**	0.358
	NV1	58	27.75	21.95	28	19.50	13.87	1.820	0.072	0.418
	NV2	60	23.80	18.36	28	14.38	12.95	2.444	0.017*	0.559
	NV3	60	20.99	16.05	28	19.72	14.77	0.354	0.724	0.081
Circuity (CR)	All phases	174	1.09	0.10	83	1.05	0.06	3.425	0.001***	0.449
	NV1	55	1.12	0.11	28	1.03	0.05	3.602	0.001***	0.954
	NV2	60	1.09	0.09	28	1.05	0.04	2.315	0.023*	0.514
	NV3	59	1.06	0.09	27	1.05	0.08	0.116	0.908	0.115

Table A2. The detailed correlation analysis results between scale scores and time cost ($^{*}p < 0.05$, FDR-corrected).

Scale	Question	*r*	*p*
SBSOD	Overall	−0.282	0.026*
	1. I am good at giving directions.	−0.218	0.089
	2. I seldom forget where I put things.	0.120	0.355
	3. I am good at judging distances.	−0.126	0.329
	4. I have a good sense of direction.	−0.209	0.103
	5. I tend to think about my surroundings in terms of cardinal directions (e.g. north, south, east, west).	−0.240	0.060
	6. I get lost hard in an unfamiliar city.	−0.164	0.201
	7. I enjoy looking at maps.	−0.214	0.095
	8. I have no difficulty understanding directions.	−0.252	0.049
	9. I am good at reading maps.	−0.336	0.008
	10. When I am a passenger in a car, I usually remember the route.	−0.066	0.610
	11. I enjoy giving directions.	−0.172	0.181
	12. Knowing where I am is important to me.	−0.250	0.050
	13. On long trips, I seldom let someone else take charge of navigation.	−0.137	0.288
	14. I usually remember a new route after walking it once.	−0.336	0.008
	15. I have a good mental map of my environment.	−0.318	0.012
NASA-TLX	Overall	0.358	0.001*
	Mental Demand	0.180	0.100
	Physical Demand	0.134	0.221
	Temporal Demand	0.253	0.019
	Performance	0.287	0.008*
	Effort	0.211	0.053
	Frustration Level	0.222	0.042

Table A3. Correlations between relative theta power and NASA-TLX scores, including its six components (*$p < 0.05$, **$p < 0.01$, FDR-corrected).

Electrode	TLX score	Mental demand	Physical demand	Temporal demand	Performance	Effort	Frustration level
AF3	0.104	0.061	0.303*	0.098	−0.129	0.065	0.167
AF4	0.050	0.095	0.324*	−0.174	−0.061	0.106	0.088
C3	0.093	0.018	0.387**	−0.048	−0.016	0.084	0.153
C4	0.100	0.122	0.332*	−0.110	−0.057	0.150	0.117
CP1	0.024	0.042	0.267	−0.046	−0.119	0.061	0.054
CP2	0.026	−0.018	0.307*	−0.080	−0.069	0.087	0.076
CP5	0.034	0.009	0.317*	−0.177	0.010	0.036	0.139
CP6	0.041	0.047	0.261	−0.033	−0.106	0.064	0.081
Cz	−0.005	−0.035	0.298*	−0.105	−0.099	0.018	0.123
F3	0.102	0.074	0.280	0.038	−0.103	0.110	0.142
F4	0.035	0.027	0.361*	−0.036	−0.132	0.059	0.080
F7	0.069	0.002	0.354*	0.011	−0.075	0.030	0.156
F8	0.143	0.082	0.397**	0.074	−0.080	0.081	0.196
FC1	0.088	0.044	0.307*	0.047	−0.094	0.034	0.175
FC2	0.055	0.012	0.256	−0.010	−0.097	0.115	0.098
FC5	0.088	0.048	0.368*	0.049	−0.113	0.057	0.134
FC6	0.151	0.153	0.324*	0.012	−0.078	0.123	0.191
Fp1	0.075	0.012	0.182	0.060	−0.067	0.004	0.212
Fp2	0.133	0.037	0.323*	0.026	−0.007	0.062	0.245
Fz	0.101	0.039	0.391**	−0.047	−0.024	0.057	0.192
O1	0.056	−0.048	0.423**	−0.060	0.055	−0.060	0.157
O2	−0.036	−0.025	0.320*	−0.167	−0.102	0.056	0.008
Oz	−0.047	−0.048	0.428**	−0.179	−0.104	−0.022	0.048
P3	0.115	0.033	0.341*	−0.043	0.014	0.118	0.164
P4	0.077	0.039	0.305*	−0.054	−0.050	0.074	0.163
P7	0.051	0.004	0.380**	−0.131	−0.011	0.039	0.149
P8	0.069	0.056	0.270	−0.039	−0.089	0.070	0.159
PO3	0.048	−0.024	0.424**	−0.094	−0.016	−0.013	0.173
PO4	−0.005	−0.018	0.347*	−0.145	−0.081	0.045	0.071
Pz	−0.077	−0.110	0.308*	−0.167	−0.085	−0.010	0.020
T7	0.074	0.041	0.408**	−0.065	−0.081	0.076	0.147
T8	0.092	0.001	0.342*	0.040	−0.035	0.036	0.163

Table A4. Interaction effect of strategy×route on relative theta PSD at the whole-brain level (*$p < 0.05$, FDR-corrected).

Electrode	F	p	f	Electrode	F	p	f
AF3	3.153	0.045	0.123	CP5	6.271	0.002*	0.280
AF4	6.987	0.001*	0.241	CP1	3.993	0.020*	0.211
Fp1	1.806	0.167	0.114	CP2	1.877	0.155	0.148
Fp2	5.493	0.005*	0.182	CP6	1.705	0.184	0.120
F7	3.750	0.025*	0.200	P7	3.306	0.038	0.185
F3	1.459	0.235	0.118	P3	1.844	0.161	0.171
Fz	4.237	0.016*	0.204	Pz	5.411	0.005*	0.247
F4	7.116	0.001*	0.298	P4	2.763	0.065	0.182
F8	5.385	0.005*	0.226	P8	2.262	0.106	0.116
FC5	3.771	0.024*	0.178	PO3	5.748	0.004*	0.287
FC1	0.353	0.703	0.087	PO4	4.437	0.013*	0.224
FC2	1.311	0.272	0.133	O1	1.768	0.173	0.196
FC6	3.757	0.025*	0.211	Oz	1.429	0.242	0.152
C3	2.063	0.129	0.183	O2	2.404	0.093	0.201
Cz	0.768	0.465	0.126	T7	4.879	0.008*	0.212
C4	4.139	0.017*	0.206	T8	3.853	0.023*	0.183